Vol. 74: 43–66, 2017
https://doi.org/10.3354/cr01484

CLIMATE RESEARCH
Clim Res

Published online November 2

Sensitivity of Indian summer monsoon simulation to physical parameterization schemes in the WRF model

J. V. Ratnam[1,*], Swadhin K. Behera[1], R. Krishnan[2], Takeshi Doi[1], Satyaban B. Ratna[3]

[1]Application Laboratory, JAMSTEC, Yokohama 2360001, Japan
[2]Center for Climate Change Research, IITM, Pune 411008, India
[3]Climatic Research Unit, School of Environmental Sciences, University of East Anglia, Norwich NR4 7TJ, UK

ABSTRACT: A set of 17 experiments, using various combinations of physical parameterization schemes in the Weather Research and Forecasting (WRF) model, were carried out to choose a combination suitable for simulating the Indian summer monsoon. The model experiments, forced with the ERA-Interim reanalysis data, were at 30 km horizontal resolution. The WRF model experiments were initialized on 1 May of each year and integrated until 30 September to cover the entire monsoon season for the years 1982 to 2013. The results indicate that the simulated Indian summer monsoon precipitation and 2 m air temperature are sensitive to the physical parameterization schemes in the WRF model and that choosing the correct combination of physical parameterization schemes is essential for simulating the Indian summer monsoon realistically. Our analysis shows that a model setup with the Kain–Fritsch cumulus scheme, a radiation package with the Dudhia shortwave and Rapid Radiative Transfer Model longwave schemes, the Yonsei State University planetary boundary layer scheme, the WRF Single-Moment 3-class microphysics scheme, the revised MM5 Monin-Obukhov surface layer scheme, and the Unified Noah land surface model is suitable for simulating the precipitation realistically. The model setup with a combination of these physical parameterization schemes was found to have smaller biases and root mean square errors in the simulated precipitation, along with a realistic simulation of intraseasonal and interannual variability of precipitation. The results of this study will be useful to researchers and forecasters using the WRF model to improve the Indian summer monsoon simulations/forecasts over the Indian region.

KEY WORDS: Regional climate model · Intra-seasonal variability · Inter-annual variability

1. INTRODUCTION

As is well known, the Indian subcontinent receives most of its precipitation during the boreal summer season from June to September (JJAS). The agro-based economy of the country is dependent on precipitation during the season, and forecasting the seasonal precipitation is beneficial to the economy of the country. Precipitation over India during the boreal summer season exhibits variability at both intraseasonal and interannual times scales. The intraseasonal variations in precipitation over India are marked with phases of high and low monsoon activity known as the active and break spells in monsoon (Ramamurthy 1969, Raghavan 1973, Krishnan et al. 2000, Annamalai & Slingo 2001, Goswami 2005, Rajeevan et al. 2010). The intraseasonal variability or intraseasonal oscillation of the monsoon precipitation has preferred periodicities of 10–20 d (Krishnamurti & Bhalme 1976, Murakami 1976, Krishnamurti & Ardunay 1980, Chen & Chen 1993) and 30 to 60 d (Krishnamurti et al. 1985, Murakami et al. 1984,

*Corresponding author: jvratnam@jamstec.go.jp

Publisher: Inter-Research · www.int-res.com

Nakazawa 1986, Goswami 2005). The intraseasonal oscillation of precipitation affects the seasonal mean precipitation (Goswami & Ajayamohan 2001) and hence the interannual variability of the boreal summer precipitation over India. The interannual variability in precipitation over India during the boreal summer season is affected by various climate modes such as the El Niño-Southern Oscillation (ENSO) and the Indian Ocean Dipole (IOD; Behera et al. 1999, Saji et al. 1999, Krishnan & Swapna 2009, Krishnan et al. 2011).

The global models used to simulate the Indian summer monsoon are usually of coarser resolution and do not capture regional features realistically. The technique of dynamical downscaling using regional climate models (RCMs; Dickinson et al. 1989, Giorgi & Bates 1989) is often used to downscale the global model simulations over India with the assumption that the better representation of orography and land-use characteristics in a high-resolution RCM can improve intraseasonal and interannual precipitation simulations. However, RCM simulations are affected by systematic biases in the RCMs, as well by the biases in the lateral boundary conditions provided by the global models. The systematic biases in RCMs are generally due to limitations of the physical parameterization schemes used to represent the physical processes in the models. An evaluation of RCMs to find a suitable combination of physical parameterization schemes can potentially reduce biases in the RCM simulations. In this study, we undertake such an evaluation of physical parameterization schemes in an RCM, the Weather Research and Forecasting (WRF; Skamarock et al. 2008) model, in simulating the Indian summer monsoon precipitation. The WRF model, which has an option to choose a number of physical parameterization schemes, provides an excellent modeling platform to carry out such a study.

A number of studies have been carried out using the RCMs to simulate the spatial and temporal features of the Indian summer monsoon at intraseasonal and interannual time scales (Bhaskaran et al. 1996, Jacob & Podzum 1997, Juang et al. 1997, Vernekar & Ji 1999, Ratnam & Kumar 2005, Dash et al. 2006, 2015, Ratnam & Cox 2006, Ratnam et al. 2009, Mukhopadhyay et al. 2010, Lucas-Picher et al. 2011, Bhaskar Rao et al. 2013, Srinivas et al. 2013, Vellore et al. 2014, Raju et al. 2015, Maharana & Dimri 2016, Umakanth et al. 2016). Using a regional climate model at 50 km resolution, which was driven by the United Kingdom Meteorological Office Unified Model (UM) global model output, Bhaskaran et al. (1996) found that the RCM improved the UM-simulated precipitation due to its higher horizontal resolution. They also found the RCM simulation to be insensitive to the size of the domain used in simulating the Indian summer monsoon. Several studies have shown that RCMs are capable of realistically simulating the Indian summer monsoon precipitation at seasonal (Jacob & Podzum 1997, Vernekar & Ji 1999) as well as at subseasonal (Maharana & Dimri 2016, Umakanth et al. 2016) time scales. However, the simulated precipitation has been found to be sensitive to the cumulus parameterization schemes used in the RCMs (Ratnam & Kumar 2005, Dash et al. 2006, Mukhopadhyay et al. 2010, Srinivas et al. 2013, Raju et al. 2015, Umakanth et al. 2016) at both seasonal and sub-seasonal time scales. A few studies, such as that of Shrivastava et al. (2014), highlight the importance of choosing a suitable combination of parameterization schemes within the WRF model to simulate the features over the Indian region. The sensitivity of the WRF model to the combination of cumulus, radiation, planetary boundary layer, and land use physical parameterization schemes in an RCM when simulating the Indian summer monsoon has not yet been studied, though such efforts have been made to study the climates of Australia (Evans et al. 2012, Kala et al. 2015), Spain (Argueso et al. 2011), Europe (Mooney et al. 2013), China (Yuan et al. 2012), and South Africa (Crétat et al. 2012). In this study, we attempt to fill this gap. The aim of this study is to find a combination of physical parameterization schemes in the WRF model suitable for simulating the Indian summer monsoon realistically.

2. MODEL AND METHODOLOGY

We used the WRF model (Advanced Research WRF; ARW) version 3.8.1 for the dynamical downscaling of ERA-Interim reanalysis data (Dee et al. 2011). The WRF model with 30 km horizontal resolution and 30 vertical levels extending from the surface to 50 hPa, covering the region 4.8° to 40.3° N, 61.1° to 98.8 E, was used in this study. We used 9 grid points in the relaxation zone in the lateral boundaries to provide a smooth transition between the prescribed lateral boundary conditions (in this case ERA-Interim reanalysis data) and the WRF simulations. A w-Raleigh damping with a damping coefficient of 0.2 was prescribed at the top of the atmosphere to damp unrealistic reflection of waves from the model top. This option can be important over high topography

(Dudhia 2016) such as the Himalayas and the Western Ghats. A time step of 90 s was used for the model runs. The radiation schemes were called at an interval of 30 min, and the Kain–Fritsch cumulus scheme (Kain 2004) was called at a 5 min interval. The Kain–Fritsch (KF) scheme is based on convective available potential energy (CAPE) closure. Once a grid point is active, sufficient time should be given for the CAPE to be removed and before another call to the scheme is made. Frequent calls to the Kain–Fritsch scheme often leads to spurious results (Correia et al. 2008). All the other physical parameterization schemes were called at every time step. A total of 17 experiments were carried out using a combination of various physical parameterization schemes in the WRF model. These experiments were provided with boundaries from the ERA-Interim reanalysis data. The WRF model experiments with the ERA-Interim reanalysis boundaries serve 2 purposes: (1) to estimate the limits of improvement we can expect from dynamical downscaling, and (2) to identify a suitable combination of physical parameterization schemes to simulate the Indian summer monsoon.

The 17 experiments (EXPT1 to EXPT17), using a combination of various physical parameterization schemes to simulate the Indian summer monsoon, are listed in Table 1. The experiments were designed to validate 2 cumulus parameterization schemes: (1) the Betts-Miller-Janjic scheme (BMJ; Betts & Miller 1986, Janjic 1994) and (2) the KF (Kain 2004) scheme; 4 shortwave radiation schemes: (1) the Dudhia scheme (Dudhia 1989), (2) the Rapid Radiative Transfer Model for GCMs (RRTMG; Iacono et al. 2008), (3) the Community Atmospheric Model (CAM; Collins et al. 2004), and (4) the Goddard shortwave scheme (Chou & Suarez 1999); 3 longwave radiation schemes: (1) the Rapid Radiative Transfer Model (RRTM; Mlawer et al. 1997), (2) the Rapid Radiative Transfer Model for GCMs (RRTMG; Iacono et al. 2008), and (3) CAM (Collins et al. 2004); 2 planetary boundary layer (PBL) schemes: (1) the Yonsei State University (YSU; Hong et al. 2006) and (2) the Asymmetric Convection Model 2 scheme (ACM2; Pleim 2007); 2 microphysical schemes: (1) the WRF Single-Moment 3-class (WSM3; Hong et al. 2004) and (2) the WRF Single-Moment 5-class (WSM5; Hong et al. 2004); 2 surface layer schemes: (1) the revised MM5 similarity scheme (MSS; Paulson 1970) and (2) the Pleim–Xiu scheme (PX; Pleim 2006); and 3 land surface models (LSM): (1) the Unified Noah LSM (Tewari et al. 2004), (2) the Pleim–Xiu (PX LSM; Pleim & Xiu 2003), and (3) the thermal diffusion scheme (Dudhia 1996). Dudhia (2016) gives an excellent description of the physical parameterization schemes in the WRF model in addition to the WRF (ARW) model website. The sets of experiments testing the sensitivity of the WRF model simulation to physical parameterization schemes are shown in Table 2. Matching symbols along a row indicate the sets of experiments compared to test the sensitivity of the model simulation to the physical scheme given in the first column of the row. For example, the pairs of experiments EXPT1 and EXPT4, EXPT2 and EXPT5,

Table 1. List of WRF model experiments. SW rad: shortwave radiation; LW rad: longwave radiation; PBL: planetary boundary layer

	Cumulus	SW rad	LW rad	PBL	Microphysics	Surface layer	Land surface
EXPT1	BMJ	Dudhia	RRTM	YSU	wsm3	MSS	Unified Noah LSM
EXPT2	BMJ	Dudhia	RRTM	ACM2	wsm3	MSS	Unified Noah LSM
EXPT3	BMJ	RRTMG	RRTMG	YSU	wsm3	MSS	Unified Noah LSM
EXPT4	KF	Dudhia	RRTM	YSU	wsm3	MSS	Unified Noah LSM
EXPT5	KF	Dudhia	RRTM	ACM2	wsm3	MSS	Unified Noah LSM
EXPT6	KF	RRTMG	RRTMG	YSU	wsm3	MSS	Unified Noah LSM
EXPT7	KF	RRTMG	RRTMG	ACM2	wsm3	MSS	Unified Noah LSM
EXPT8	KF	RRTMG	RRTMG	ACM2	wsm5	MSS	Unified Noah LSM
EXPT9	KF	CAM	CAM	YSU	wsm3	MSS	Unified Noah LSM
EXPT10	KF	CAM	CAM	ACM2	wsm3	MSS	Unified Noah LSM
EXPT11	KF	CAM	CAM	ACM2	wsm5	MSS	Unified Noah LSM
EXPT12	KF	CAM	RRTM	YSU	wsm3	MSS	Unified Noah LSM
EXPT13	KF	Goddard	RRTM	YSU	wsm3	MSS	Unified Noah LSM
EXPT14	KF	Dudhia	RRTM	ACM2	wsm3	PX	Unified Noah LSM
EXPT 15	KF	Dudhia	RRTM	ACM2	wsm3	PX	PX LSM
EXPT16	KF	Dudhia	RRTM	ACM2	wsm3	MSS	Thermal diffusion
EXPT17	KF	Dudhia	RRTM	ACM2	wsm5	MSS	Unified Noah LSM

Table 2. The sets of model experiments testing the physical parameterization schemes in the WRF model. Matching symbols along a row indicate that the models differ only in the physical parameterization scheme given in the first column of the row. PBL: planetary boundary layer; SW rad: shortwave radiation; LW rad: longwave radiation

	Experiment No.																
	1	2	3	4	5	6	7	8	9	10	11	12	13	14	15	16	17
Cumulus	X	+	*	X	+	*											
PBL	X	X		*	*	+	+		•	•							
SW rad				X								X	X				
LW rad									X			X					
LW+SW	+		+	X		X											
Microphysics					+		X	X		*	*						+
Surface layer					X									X			
Land surface					X									+	+	X	

and EXPT3 and EXPT6, which differ only in the cumulus scheme, are compared to test the sensitivity of the model simulation to the cumulus scheme used. Similarly, the other rows in Table 2 list the sets of experiments testing the various physical schemes in the model.

The initial and lateral boundaries for the 17 experiments were derived from the ERA-Interim reanalysis data at a horizontal resolution of 0.75° × 0.75°. The WRF model runs were for the period 1982 to 2013, with the model initialized on 1 May of each year and integrated until 30 September to cover the entire monsoon season.

The WRF model-simulated precipitation and 2 m air temperature were validated using the high-resolution precipitation (Pai et al. 2014) and 2 m air temperature (Srivastava et al. 2009) dataset of the India Meteorological Department (IMD). The IMD precipitation data is at a resolution of 0.25° × 0.25° and the 2 m air temperature data is at 1° × 1° resolution.

The El Niño events used for the composite analysis were identified from the historical information available from the Climate Prediction Center (CPC), USA. To identify IOD events, we used the monthly IOD index obtained from the Japan Agency for Marine-Earth Science and Technology (JAMSTEC), Japan. To ensure that the IOD events had sufficient strength in the JJAS season to influence the Indian summer monsoon, we took a running average of the monthly index for the seasons June to August (JJA), July to September (JAS), August to October (ASO), and September to November (SON) and normalized the index for a season with its SD. We considered years as IOD years when the index was above 0.9 SD in at least 3 consecutive seasons of JJA, JAS, ASO, and SON.

3. RESULTS

3.1. Seasonal mean precipitation and 2 m air temperature

3.1.1. Sensitivity to cumulus parameterization schemes

The IMD observed precipitation (Fig. 1a), averaged over the JJAS season from 1982 to 2013, exhibits heterogeneity in the spatial distribution of precipitation over the Indian landmass, with precipitation >10 mm d^{-1} in the northeast and along the west coast (along the Western Ghats), and with precipitation of <2 mm d^{-1} in the northwest and the south (Fig. 1a). The precipitation over central India is in the range of 5 to 15 mm d^{-1} during the season with a propensity to higher precipitation in the eastern parts (Fig. 1a). The WRF model experiments were able to capture the spatial distribution of the mean precipitation realistically, though they differ in the magnitude of simulated seasonal precipitation (Fig. 1b–r).

The model-simulated precipitation was often found to be sensitive to the cumulus parameterization scheme used in the model due to the convective nature of the Indian summer monsoon precipitation. The results of the pairs of experiments EXPT1 (Fig. 1b) and EXPT4 (Fig. 1e), EXPT2 (Fig. 1c) and EXPT5 (Fig. 1f), and EXPT3 (Fig. 1d) and EXPT6 (Fig. 1g), which differ only in the cumulus scheme (Table 2), were compared to test the sensitivity of the WRF-simulated precipitation to the cumulus scheme used in the model. Not surprisingly, the comparison shows the model-simulated precipitation to be sensitive to the cumulus parameterization scheme, in agreement with the previous studies of Mukhopadhyay et al. (2010), Srinivas et al. (2013),

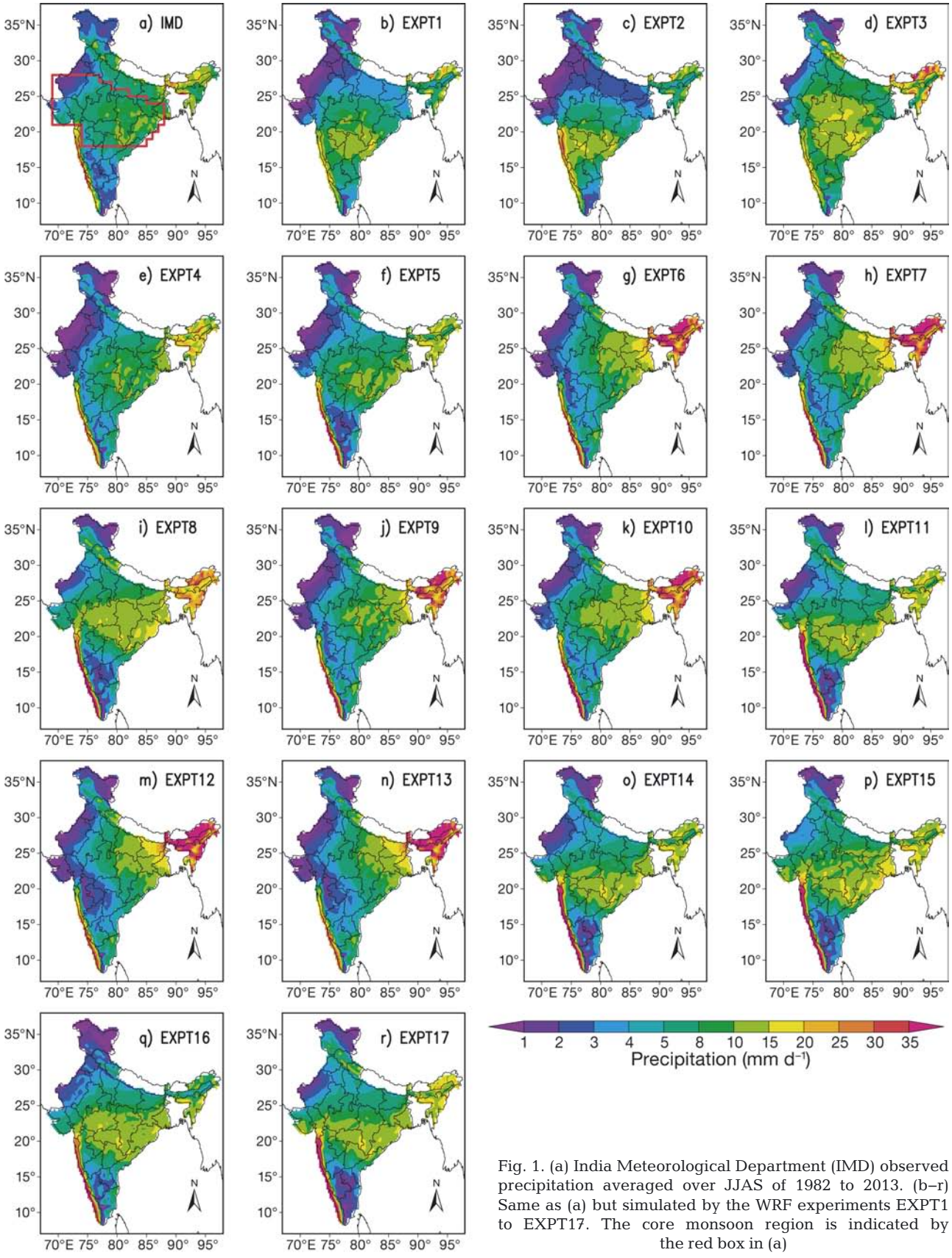

Fig. 1. (a) India Meteorological Department (IMD) observed precipitation averaged over JJAS of 1982 to 2013. (b–r) Same as (a) but simulated by the WRF experiments EXPT1 to EXPT17. The core monsoon region is indicated by the red box in (a)

Raju et al. (2015), and Umakanth et al. (2016). We calculated the root mean square error (RMSE; Fig. 2) and model biases (Fig. 3) to quantify the errors and biases in the precipitation simulated by the model experiments. Comparing the RMSE and significant biases in the simulated precipitation for the pairs of model experiments, EXPT1; (Figs. 2a & 3a) and EXPT4 (Figs. 2d & 3d), EXPT2 (Figs. 2b & 3b) and EXPT5 (Figs. 2e & 3e), and EXPT3 (Figs. 2c & 3c) and EXPT6 (Figs. 2f & 3f)), it is evident that the model experiments with the KF scheme (EXPT4, EXPT5, and EXPT6) outperform the model experiments with the BMJ scheme (EXPT1, EXPT2, and EXPT3) in simulating precipitation over the Indian landmass during the JJAS season. The model experiments with the KF scheme have smaller biases and RMSE compared to those with the BMJ cumulus parameterization scheme. The BMJ scheme experiments EXPT1 (Fig. 3a) and EXPT2 (Fig. 3b) have significant dry biases over northern parts of India and wet biases over the southern parts with magnitudes exceeding 3 mm d^{-1}, whereas the KF scheme experiments EXPT 4 (Fig. 3d) and EXPT5 (Fig. 3e) have comparatively smaller biases over the Indian landmass during the JJAS season. EXPT3 (BMJ; Fig. 3c) simulated precipitation in >3 mm d^{-1} over the entire landmass, whereas EXPT6 (KF; Fig. 3f) has smaller biases over the core monsoon region (box in Fig. 1a; Rajeevan et al. 2010).

The JJAS seasonal mean 2 m air temperatures are >31°C over parts of northwest India, with temperatures around 27°–31°C over the core monsoon region (Fig. 4a). The regions in the northwest and southern parts receive very little precipitation during the season (Fig. 1a), leading to high 2 m air temperatures (Fig. 4a). Similar to precipitation, the 2 m air temperature simulations of the pairs of experiments, EXPT1 (Fig. 4b) and EXPT4 (Fig. 4e), EXPT2 (Fig. 4c) and EXPT5 (Fig. 4f), and EXPT3 (Fig. 4d) and EXPT6 (Fig. 4g), were compared to test the sensitivity to the cumulus scheme used in the model. EXPT1 (Fig. 4b), EXPT4 (Fig. 4e), EXPT2 (Fig. 4c), and EXPT5 (Fig. 4f) have warm (cool) biases over the northern (southern) parts of India corresponding to the dry (wet) bias in precipitation over the regions (Fig. 3a,d,b,e, respectively). However, the differences in the 2 m air temperature biases between the experiments are not as prominent as those for precipitation. It is interesting to note that EXPT3, which has a wet bias in simulated precipitation over most parts of India (Fig. 3c) and EXPT6, also with a wet bias over the northern parts of India (Fig. 3f), have a warm bias in the simulated 2 m air temperatures (Fig. 4d,g).

We calculated the biases in the vertically integrated (from surface to 300 hPa) moisture fluxes and its divergence to understand the causes of the differences in the precipitation simulated by the KF and BMJ schemes. Fig. 5 shows significant biases in the simulated vertically integrated moisture fluxes (vectors) and their divergence (shaded) compared to the ERA-Interim estimated fluxes and divergence. The fluxes are averaged over the JJAS season for all the years from 1982 to 2013. EXPT1 (Fig. 5a) and EXPT2 (Fig. 5b), which use the BMJ cumulus parameterization, simulated a cyclonic bias in the moisture fluxes over the southern Bay of Bengal region leading to transport of moisture into southern parts of India. A region of moisture flux convergence bias (Fig. 5a,b) is seen over the southern parts of India leading to the wet bias in precipitation over the region in these experiments (Fig. 3a,b). The moisture flux bias is divergent over northern parts of India, leading to an underestimation of precipitation (Fig. 3a,b). EXPT4 (Fig. 5d) and EXPT5 (Fig. 5e), which use the KF scheme, have smaller biases in the vertically integrated moisture fluxes leading to smaller biases in the simulated precipitation compared to EXPT1 and EXPT2. A cyclonic bias in the moisture flux is simulated in EXPT3 (Fig. 5c) leading to a wet bias over the whole Indian landmass (Fig. 3c). Similarly, the precipitation biases in EXPT6 (Fig. 3f) can be explained by the biases in the moisture fluxes (Fig. 5f).

The spatial distribution of the tropical precipitation, due to its convective nature, can be explained by the tropospheric moist static energy (MSE; Srinivasan & Smith 1996). Analyzing the biases in the simulated MSE by different WRF model experiments can help to clarify the precipitation biases simulated by the model. The biases in the seasonal vertically averaged (from 1000 to 300 hPa) MSE simulated by all the model experiments is shown in Fig. 6a–q. The model experiments with the BMJ cumulus scheme, EXPT1 (Fig. 6a), EXPT2 (Fig. 6b), and EXPT3 (Fig. 6c), simulated a more unstable atmosphere with positive biases in MSE exceeding 2 kJ kg^{-1} over the core monsoon region. EXPT1 and EXPT2, which simulated wet (dry) biases in the southern (northern) parts of India, simulated an unstable (stable) atmosphere with positive (negative) biases in the vertically averaged MSE over the regions. EXPT3 (Fig. 6c) simulated an unstable model climate over the Indian landmass which resulted in positive biases in the precipitation (Fig. 3c). The corresponding model experiments with the KF cumulus scheme, EXPT4, EXPT5, and EXPT6, which simulated smaller biases in precipitation, also simulated smaller biases in the vertically averaged MSE (Fig. 6d,e,f).

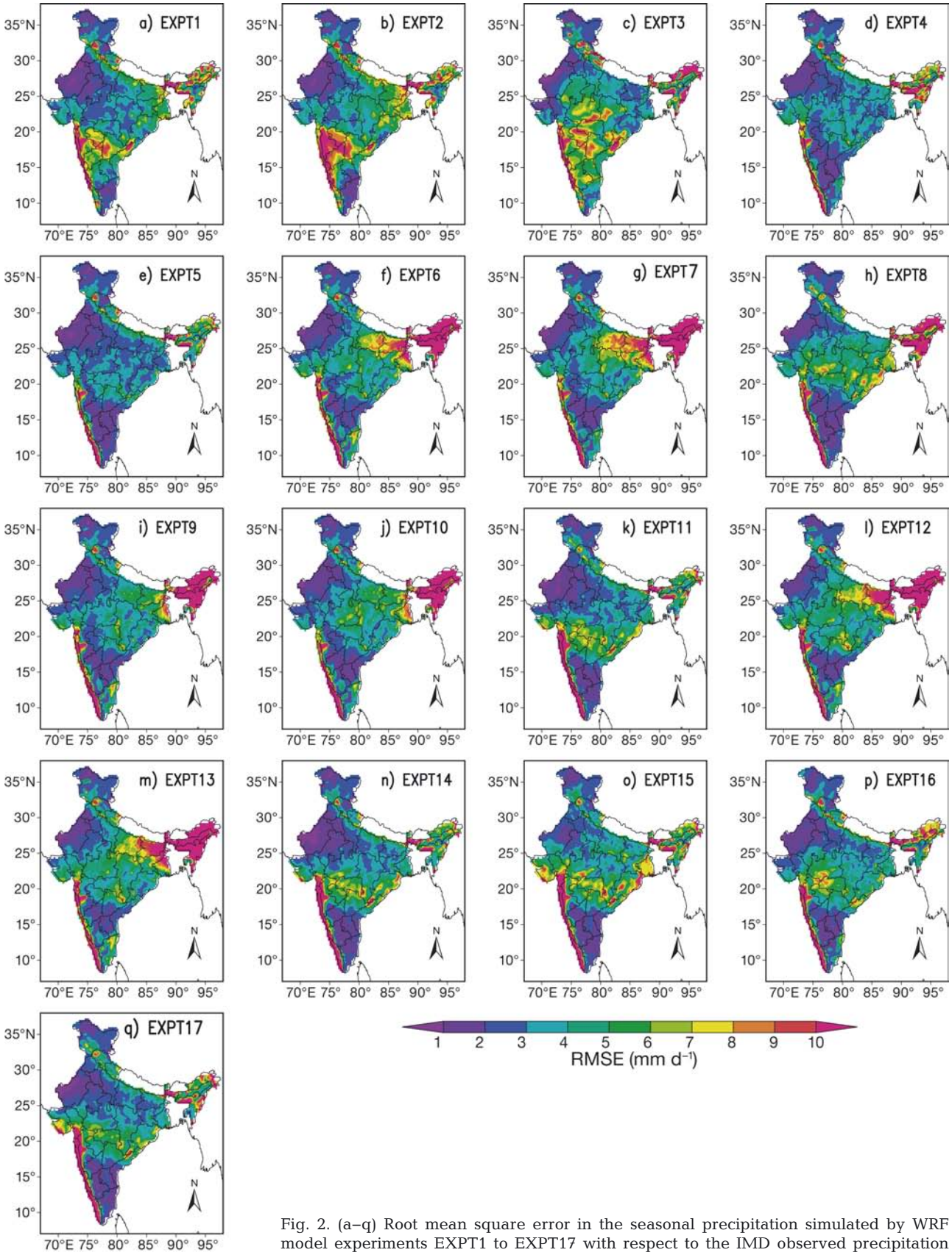

Fig. 2. (a–q) Root mean square error in the seasonal precipitation simulated by WRF model experiments EXPT1 to EXPT17 with respect to the IMD observed precipitation

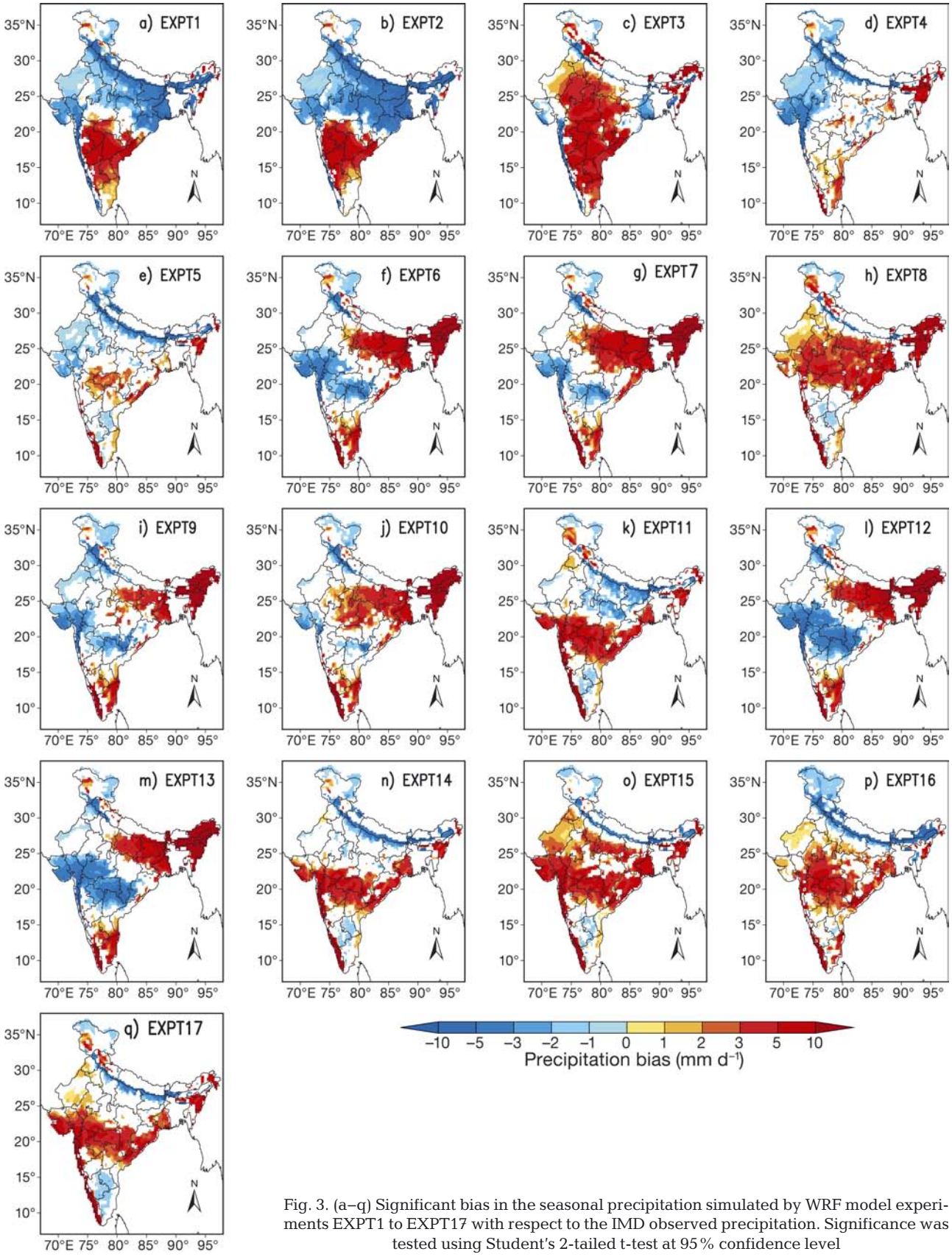

Fig. 3. (a–q) Significant bias in the seasonal precipitation simulated by WRF model experiments EXPT1 to EXPT17 with respect to the IMD observed precipitation. Significance was tested using Student's 2-tailed t-test at 95% confidence level

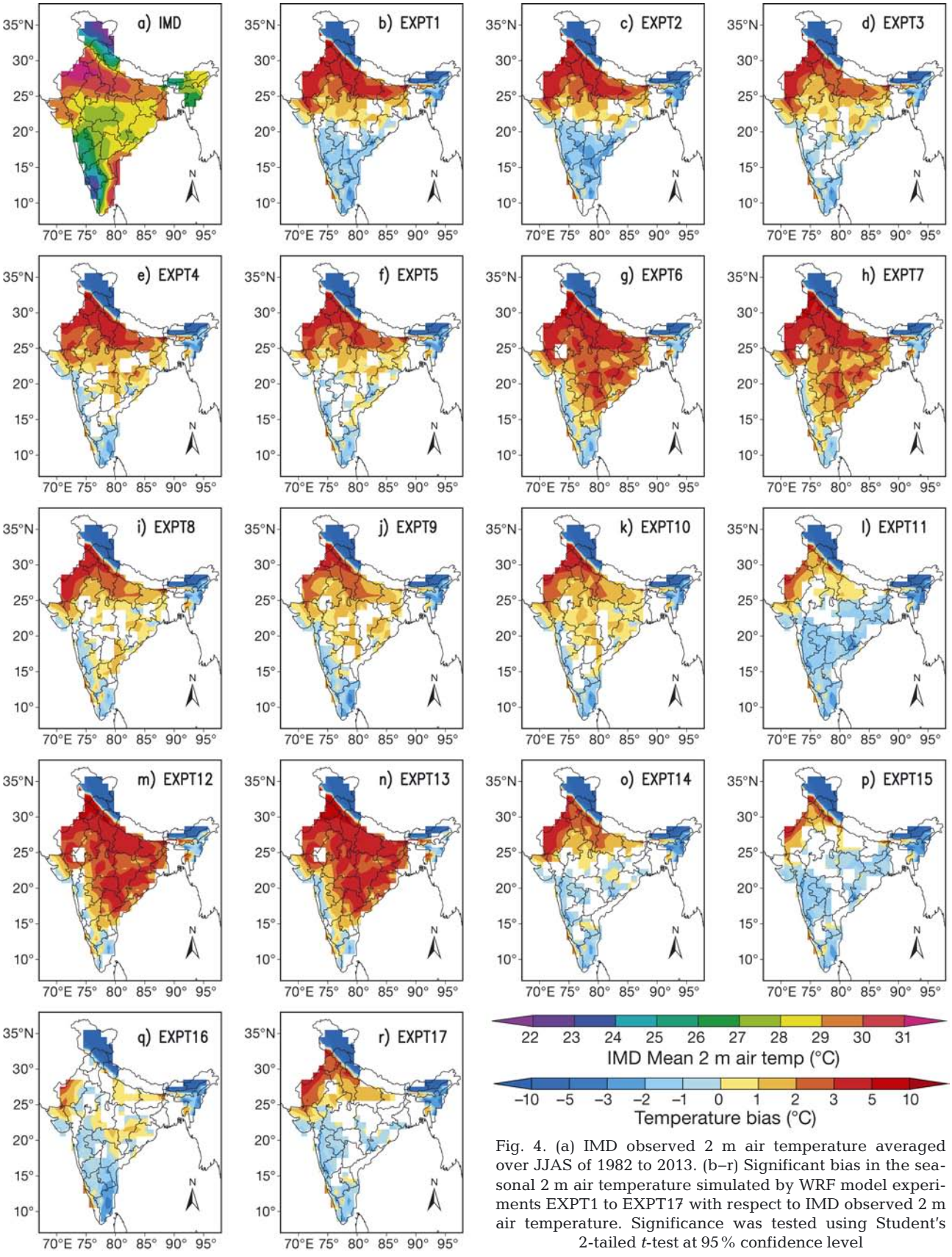

Fig. 4. (a) IMD observed 2 m air temperature averaged over JJAS of 1982 to 2013. (b–r) Significant bias in the seasonal 2 m air temperature simulated by WRF model experiments EXPT1 to EXPT17 with respect to IMD observed 2 m air temperature. Significance was tested using Student's 2-tailed *t*-test at 95 % confidence level

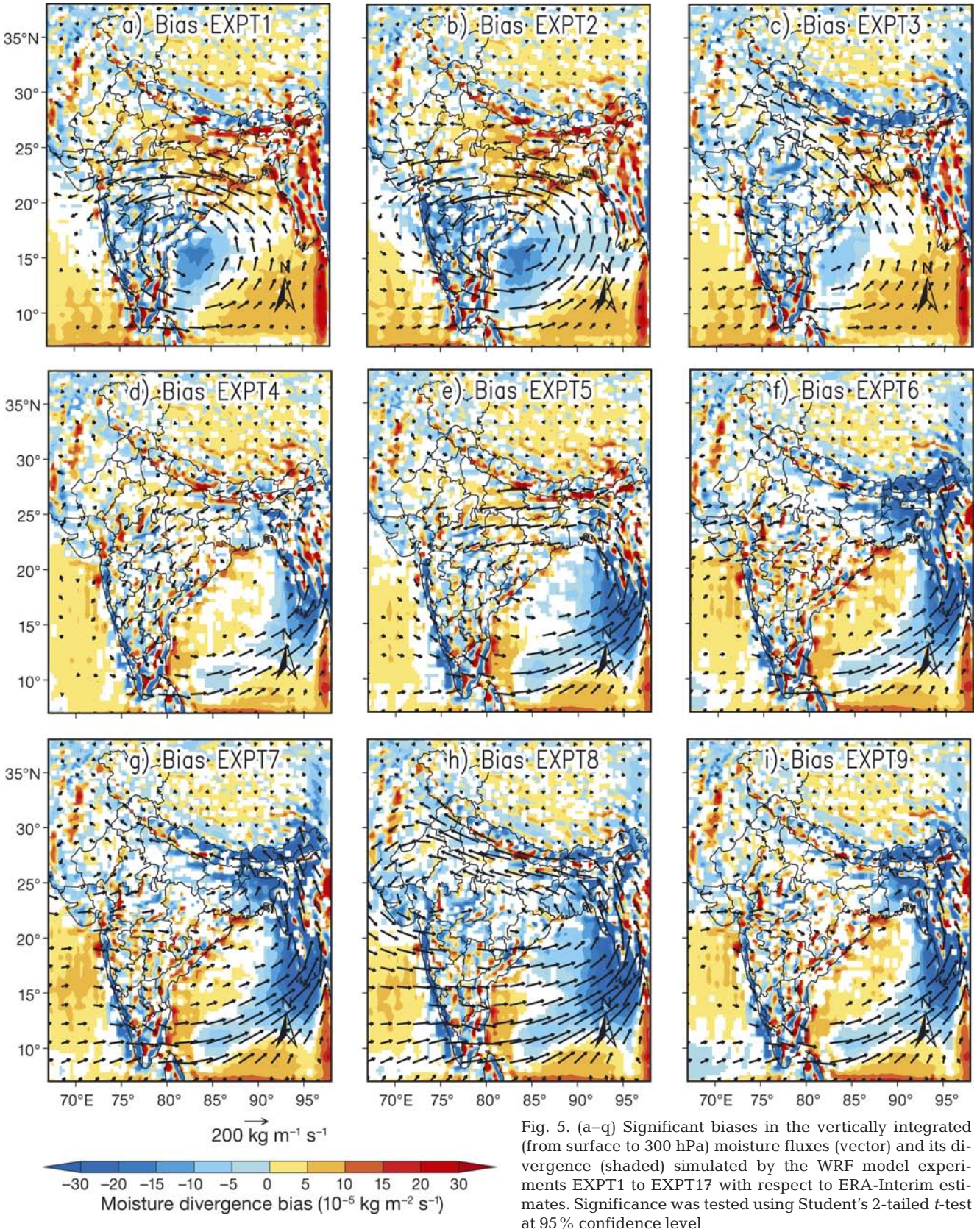

Fig. 5. (a–q) Significant biases in the vertically integrated (from surface to 300 hPa) moisture fluxes (vector) and its divergence (shaded) simulated by the WRF model experiments EXPT1 to EXPT17 with respect to ERA-Interim estimates. Significance was tested using Student's 2-tailed *t*-test at 95% confidence level

(continued on next page)

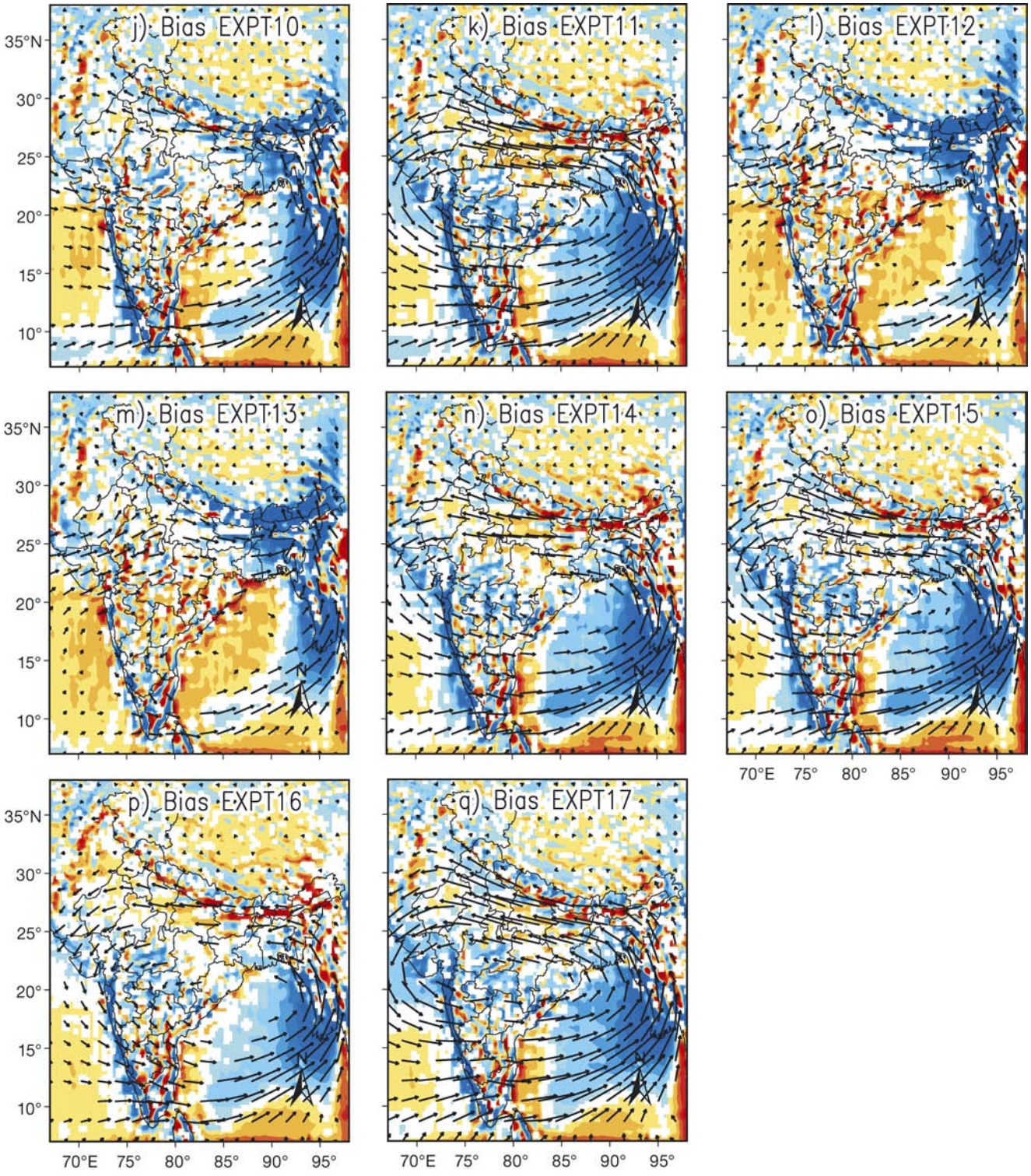

Fig. 5 (continued)

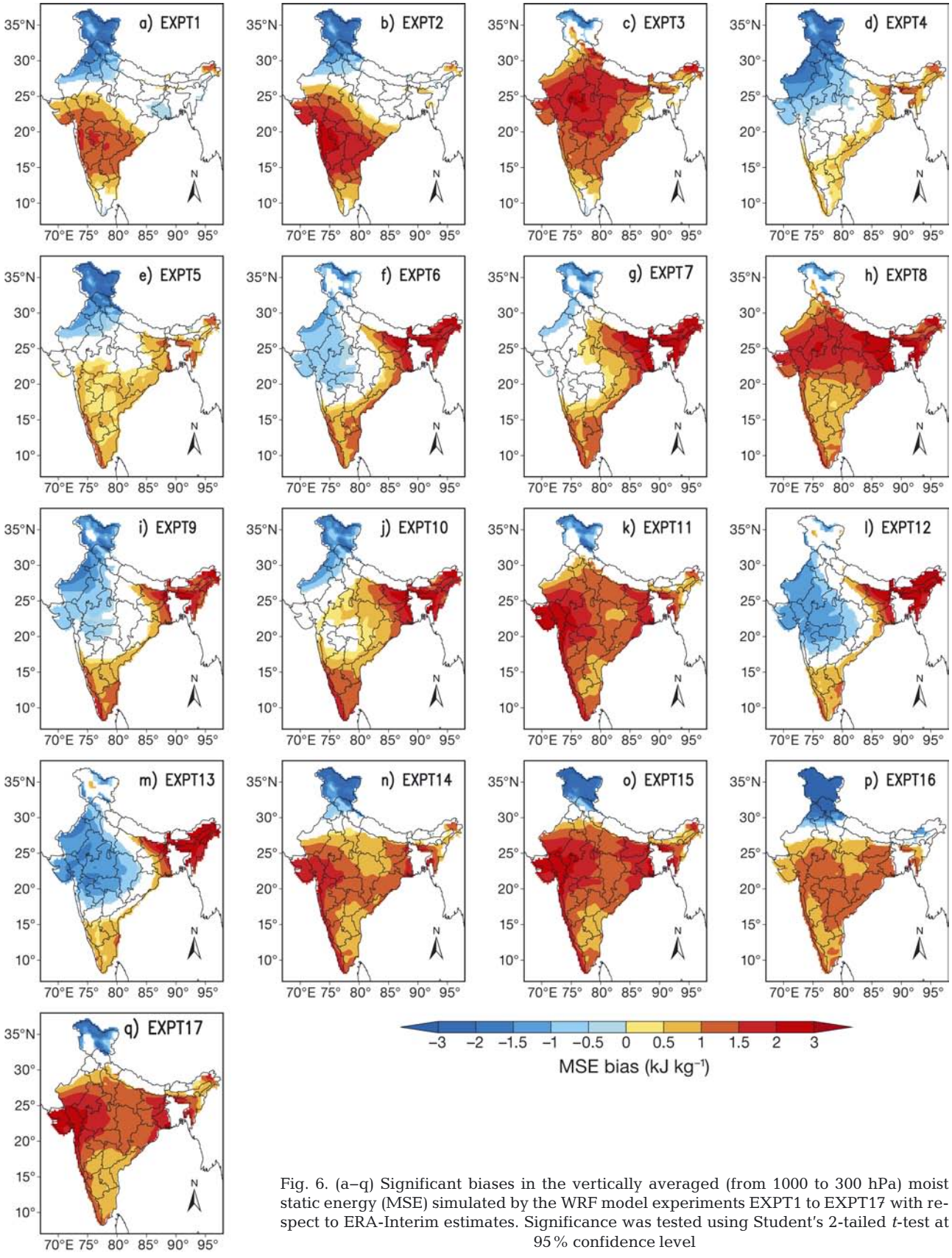

Fig. 6. (a–q) Significant biases in the vertically averaged (from 1000 to 300 hPa) moist static energy (MSE) simulated by the WRF model experiments EXPT1 to EXPT17 with respect to ERA-Interim estimates. Significance was tested using Student's 2-tailed *t*-test at 95% confidence level

Based on the above analysis, we find that the KF scheme is more suitable for simulating the Indian summer monsoon precipitation under the present model setup compared to the BMJ scheme.

3.1.2. Sensitivity to PBL schemes

The results of the pairs of experiments EXPT1 (Fig. 1b) and EXPT2 (Fig. 1c), EXPT4 (Fig. 1e) and EXPT5 (Fig. 1f), EXPT6 (Fig. 1g) and EXPT7 (Fig. 1h), and EXPT9 (Fig. 1j) and EXPT10 (Fig. 1k), which differ only in the PBL scheme used (Table 2), were compared to test the sensitivity of the model-simulated precipitation to the PBL scheme. EXPT1, EXPT4, EXPT6, and EXPT9 use the YSU scheme, whereas EXPT2, EXPT5, EXPT7, and EXPT10 use the ACM2 scheme. The precipitation simulated by EXPT1 (Fig. 1b), EXPT4 (Fig. 1e), EXPT6 (Fig. 1g), and EXPT9 (Fig. 1j) differs from that simulated by EXPT2 (Fig. 1c), EXPT5 (Fig. 1f), EXPT7 (Fig. 1h), and EXPT10 (Fig. 1k). Comparing EXPT1 and EXPT2, it can be seen that the precipitation simulated by EXPT1 has smaller RMSE (Fig. 2a) and biases (Fig. 3a) compared to those (Figs. 2b & 3b) of the precipitation simulated by EXPT2 over the Indian landmass. EXPT2 (ACM2) has dry biases >3 mm d^{-1} over the central and northern parts of India (Fig. 3b) and wet biases >3 mm d^{-1} over the southern parts of India (Fig. 3b). The dry biases over the central and northern parts of India are smaller in EXPT1 (YSU) (Fig. 3a). The cool (warm) biases in the 2 m air temperature in EXPT1 (Fig. 4b) over southern (northern) parts of India are smaller than in EXPT2 (Fig. 4c). The biases in the vertically integrated moisture flux simulated by EXPT2 (Fig. 5b) are larger than those simulated by EXPT1 (Fig. 5a). The biases in divergence (convergence) in vertically integrated moisture flux over northern (southern) parts of India are larger in EXPT2 (Fig. 5b; shaded) compared to EXPT1 (Fig. 5a), leading to larger dry (wet) biases in the northern (southern) parts of India in EXPT2 (Fig. 3b) compared to EXPT1 (Fig. 3a). Comparing the RMSE and bias in the precipitation simulated by the other pairs of experiments, EXPT4 and EXPT5 (Figs. 2d,e & 3d,e), EXPT6 and EXPT7 (Figs. 2f,g & 3f,g), and EXPT9 and EXPT10 (Figs. 2i,j & 3i,j), it is evident that the precipitation simulated with the ACM2 PBL scheme has larger RMSE and biases compared to that simulated with the YSU PBL scheme.

On comparing biases in the MSE simulated by the pairs of experiments EXPT1 (Fig. 6a) and EXPT2 (Fig. 6b), EXPT4 (Fig. 6d) and EXPT5 (Fig. 6e), EXPT6 (Fig. 6f) and EXPT7 (Fig. 6g) and EXPT9 (Fig. 6i) and EXPT10 (Fig. 6j), it is evident that the models with the ACM2 PBL scheme (EXPT2, EXPT5, EXPT7, and EXPT10) yielded a more unstable model climate compared to those with the YSU PBL scheme (EXPT1, EXPT4, EXPT6 and EXPT9), resulting in wet biases of higher magnitude in the experiments with the ACM2 PBL scheme. It is interesting to note that though the WRF model experiments are sensitive to the PBL scheme used, the differences between the experiments are not as large as those due to the different cumulus schemes.

3.1.3. Sensitivity to radiation schemes

The sensitivity of the Indian summer monsoon precipitation to the shortwave radiation schemes was tested by comparing the results of EXPT4, EXPT12, and EXPT13 (Table 2). Comparing the mean precipitation, RMSE, and biases of the precipitation simulated by EXPT4 (Figs. 1e, 2d & 3d), EXPT12 (Figs. 1m, 2l & 3l), and EXPT13 (Figs. 1n, 2m & 3m) over the Indian landmass, it can be seen that the Dudhia shortwave radiation scheme (EXPT4) generates smaller biases and RMSE compared to the CAM (EXPT12) and Goddard (EXPT13) shortwave radiation schemes. The WRF models with the CAM (EXPT12) and Goddard (EXPT13) shortwave radiation schemes have wet biases (Fig. 3l,m) >3 mm d^{-1} over the northeastern and eastern parts of central India and dry biases of >3 mm d^{-1} over the western parts of central India. However, the precipitation biases (Fig. 3l,m) and RMSE (Fig. 2l,m) simulated by EXPT12 are similar to those generated by EXPT13. The Dudhia shortwave radiation scheme (EXPT4) also has smaller biases and RMSE compared to the CAM (EXPT12) and Goddard (EXPT13) shortwave radiation schemes in simulating the 2 m air temperatures over the Indian landmass. EXPT4 (Dudhia) has a warm bias of about 1 to 2°C over the core monsoon region (Fig. 4e), while the warm biases are >2°C over most parts of the Indian landmass in EXPT12 (CAM; Fig. 4m) and in EXPT13 (Goddard; Fig. 4n). The biases in the precipitation and 2 m air temperatures simulated by EXPT12 and EXPT13 can be attributed to the cyclonic moisture flux biases in the Bay of Bengal, with moisture converging over northeast India (Fig. 5l,m). These experiments also simulate moisture transport from the Arabian Sea converging over the eastern parts of central India, which results in a wet bias over the region (Fig. 3l,m). Regions of divergent

bias are seen over parts of central and southern India in both EXPT12 and EXPT13 (Fig. 5l,m) which result in dry bias in the precipitation over the region (Fig. 3l,m). The analysis of biases in the MSE shows that the models with CAM (EXPT12) and Goddard (EXPT13) shortwave radiation schemes simulated a stable atmosphere over the core monsoon region with negative biases in the MSE (Fig. 6l,m), resulting in dry bias over the core monsoon region. EXPT4 (Fig. 6d) (Dudhia) simulated MSE with smaller biases compared to EXPT12 (Fig. 6l) and EXPT13 (Fig. 6m).

The WRF model experiment results also indicate that the model-simulated Indian summer monsoon precipitation is sensitive to the longwave radiation scheme used. Comparing the mean (Fig. 1j,m), RMSE (Fig. 2i,l) and biases (Fig. 3i,l) of EXPT9 and EXPT12, which differ in the longwave radiation scheme used (Table 2), indicates that the CAM (EXPT9; Fig. 3i) longwave radiation scheme simulates precipitation with smaller biases compared to the RRTM (EXPT12; Fig. 3l) longwave radiation scheme. The 2 m air temperatures simulated by EXPT9 (Fig. 4j) have smaller biases compared to those simulated by EXPT12 (Fig. 4m) over the Indian landmass. The differences in the precipitation and 2 m air temperatures biases between EXPT9 and EXPT12 are related to the differences in the moisture flux biases simulated by the experiments. EXPT12 simulated large convergence bias over northwestern and eastern central India, resulting in wet bias over the region (Fig. 5l). The biases in the moisture flux and its divergence simulated by EXPT9 (Fig. 5i) are smaller than those simulated by EXPT12. EXPT12 also simulated a more stable model climate with negative biases exceeding 1 kJ kg^{-1} in the MSE over the core monsoon region (Fig. 6l) compared to EXPT9, which had a negative bias of about 0.5 kJ kg^{-1} in the MSE (Fig. 6i), resulting in differences in the biases in the precipitation and 2 m air temperature.

Apart from the WRF model being sensitive to both the shortwave and the longwave radiation scheme in simulating the Indian summer monsoon precipitation and 2 m air temperatures, we find that the model results are also sensitive to the choice of radiation package (combination of shortwave and longwave radiation schemes). On comparing the mean precipitation, RMSE, and bias simulated by EXPT1 (Figs. 1b, 2a & 3a) and EXPT3 (Figs. 1d, 2c & 3c), and EXPT4 (Figs. 1e, 2d & 3d) and EXPT6 (Figs. 1g, 2f & 3f), which differ in the radiation package used (Table 2), it is evident that the RRTMG radiation package performs poorly in simulating precipitation over India, with a large wet bias of >5 mm d^{-1} and a large RMSE. In EXPT3, which used the BMJ cumulus scheme, the RRTMG radiation package simulated a wet bias of >5 mm d^{-1} over the whole of India, with a region of convergence (Fig. 5c) covering the entire landmass. In EXPT3, the RRTMG radiation package in combination with other physical schemes simulated an unstable model climate with positive biases >1.5 kJ kg^{-1} over the entire Indian landmass (Fig. 6c). However, although the RRTMG radiation package in combination with the KF cumulus scheme (EXPT6) and other physical parameterization schemes simulated higher precipitation, the region of high precipitation is confined to eastern central India (Fig. 3f), with less precipitation over the south (Fig. 3f), in agreement with the region of convergence (divergence) bias over these areas (Fig. 5f) and positive (negative) bias in the simulated MSE (Fig. 6f). These results show that the sensitivity of a model to the radiation package is dependent on the choice of other physical parameterization schemes. Comparing the precipitation and 2 m air temperatures simulated by the model experiments with the RRTMG (EXPT3, EXPT6, EXPT7, EXPT8) and CAM (EXPT9 and EXPT10) radiation packages with the model experiments with a radiation package consisting of the Dudhia shortwave radiation and RRTM longwave radiation schemes (EXPT1, EXPT2, EXPT4, EXPT5), it is clear that the latter combination outperforms the former, with smaller biases and RMSE in the simulated precipitation over the Indian landmass. The RRTMG and CAM radiation packages tend to simulate higher precipitation over central and northern parts of India.

3.1.4. Sensitivity to microphysical schemes

As seen in Table 2, the results of the pairs of experiments EXPT7 and EXPT8, EXPT10 and EXPT11, and EXPT5 and EXPT17 were compared to test the sensitivity of the simulated Indian summer monsoon precipitation to the microphysical schemes in the WRF model. On comparing the model simulated precipitation, RMSE and biases in EXPT7 (Fig. 1h, Fig 2g and Fig 3g) with WSM3 microphysical scheme with those of EXPT8 (Figs. 1i, Fig 2h, Fig 3h) with the WSM5 microphysical scheme it is found that the WSM5 scheme simulated larger biases and RMSE compared to WSM3 scheme over the landmass. Similar results were obtained on comparing the mean, RMSE and biases for the simulated precipitation in EXPT5 (Figs. 1f, 2e & 3e) with the WSM3 scheme with those of EXPT17 (Figs. 1r, 2q & 3q) with

the WSM5 scheme. The biases simulated by EXPT10 (Fig. 3j) with the WSM3 scheme are positive over the core monsoon region, whereas those simulated by EXPT11 with the WSM5 scheme (Fig. 3k) are significantly negative. However, the 2 m air temperature simulated by the WSM3 schemes in EXPT5 (Fig. 4f), EXPT7 (Fig. 4h), and EXPT10 (Fig. 4k) shows a warm bias of >2°C compared to the 1°C warm bias simulated by EXPT8 (Fig. 4i), EXPT11 (Fig. 4l) and EXPT17 (Fig. 4r), the experiments using the WSM5 microphysical scheme.

The WSM5 microphysical scheme experiments EXPT8 (Fig. 5h), EXPT11 (Fig. 5k), and EXPT17 (Fig. 5q) simulated a cyclonic bias in moisture fluxes covering the whole Indian landmass, creating a region of convergence that resulted in a wet bias in precipitation. The model experiments with the WSM3 microphysical scheme, EXPT5 (Fig. 5e), EXPT7 (Fig. 5g), and EXPT10 (Fig. 5j), simulated cyclonic bias in the moisture over the Bay of Bengal and northeast India. The model experiments with the WSM5 microphysical scheme also simulated an unstable climate with positive MSE biases covering the entire Indian landmass (Fig. 6h,k,q), resulting in wet biases in precipitation. These results indicate that the model-simulated Indian summer monsoon precipitation and 2 m air temperature are sensitive to the microphysical schemes used in the model and that the WSM3 scheme is more suitable for simulating precipitation under the present model setup.

3.1.5. Sensitivity to surface layer schemes

The surface layer schemes enable exchange of information from the atmosphere to the earth's surface for calculation by the land surface models. Choosing a suitable surface layer scheme to simulate the Indian summer monsoon precipitation and 2 m air temperatures is important. We carried out 2 experiments, the first with the MSS surface layer scheme (EXPT5) and the second with the PX surface layer scheme (EXPT14) (Table 2). The results of the comparison between EXPT5 (Fig. 1f) and EXPT14 (Fig. 1o) indicate that the simulated precipitation is sensitive to the surface layer scheme used in the model. The RMSE in the precipitation simulated with the PX scheme in EXPT14 (Fig. 2n) is larger over most parts of the core monsoon region than that in the precipitation simulated with the MSS surface layer scheme in EXPT5 (Fig. 2e). Similarly, the wet precipitation biases over the core monsoon region are larger in EXPT14 (Fig. 3n) compared to EXPT5 (Fig. 3e). However, the 2 m air temperature biases over northern parts of India have smaller warm biases in EXPT14 compared to EXPT5 due to the larger wet biases simulated by EXPT14.

The model experiment with the PX surface layer scheme (EXPT14; Fig. 5n) simulated a cyclonic bias in moisture fluxes covering the Bay of Bengal and the core monsoon region, resulting in a significant convergence bias over the landmass and hence the wet bias in the precipitation. EXPT5 with the MSS scheme (Fig. 5e) shows smaller biases in the moisture flux compared to EXPT14. The positive bias in the vertically averaged MSE in EXPT14 (Fig. 6n) is >1 kJ kg^{-1} over the core monsoon region, indicating that the model has simulated an unstable climate resulting in excess precipitation over the landmass. These results indicate that the simulated monsoon precipitation and 2 m air temperature are sensitive to the choice of the surface layer scheme.

3.1.6. Sensitivity to land surface schemes

The land surface schemes model the surface processes and provide the surface sensible heat flux, surface latent heat flux, upward longwave radiation, and reflected upward shortwave radiation to the atmospheric model. We carried out experiments with 3 land surface schemes, namely the Unified Noah LSM, the thermal diffusion model, and the PX land surface model, to test the sensitivity of the model precipitation to these schemes. The comparison of the pairs of experiments, EXPT5 and EXPT16 (Fig. 1f,q), and EXPT14 and EXPT15 (Fig. 1o,p), clearly reveal the importance of specifying an appropriate land surface scheme (Table 2). EXPT5 with the Unified Noah LSM has smaller biases (Fig. 3e) and RMSE (Fig. 2e) over the core monsoon region compared to EXPT16 with the thermal diffusion scheme (Figs. 2p & 3p). A precipitation bias >5 mm d^{-1} is simulated over the entire core monsoon region in EXPT16 (Fig. 3p). This excess precipitation results in a smaller warm bias of about 1°C over northern parts of India compared to the bias of over 2°C in EXPT5 (Fig. 4f) over the same region. The thermal diffusion land surface model (EXPT16) simulated an unstable model climate with positive biases in vertically averaged MSE over the entire core monsoon region (Fig. 6p) and moisture convergent biases (Fig. 5p), resulting in large wet biases over the region. Similarly, EXPT14 with the Unified Noah LSM has smaller biases (Fig. 3n) and RMSE (Fig. 2n) over the core monsoon region compared to those simulated by EXPT15 with the PX

land surface scheme (Figs. 3o & 2o). The biases in 2 m air temperature in EXPT15 (Fig. 4p) are smaller than those in EXPT14 (Fig. 4o) due to the higher wet biases simulated in EXPT15. The biases in the moisture fluxes (Fig. 5o) and MSE (Fig. 6o) also indicate a more unstable atmosphere in EXPT15 compared to EXPT14 (Figs. 5n & 6n), which explains the difference in the precipitation and 2 m air temperatures simulated by the experiments over the Indian landmass. These results indicate that the Unified Noah LSM is superior to the PX land surface model and the thermal diffusion scheme in simulating the monsoon precipitation under the present model setup.

3.1.7. Taylor diagrams

A comprehensive comparison of the model-simulated precipitation and 2 m air temperatures in the various experiments is presented in the Taylor diagram shown in Fig. 7a,b. The observed and model-simulated precipitation and 2 m air temperatures over the core monsoon region are derived from IMD observations and the model experiments. From Fig. 7a, it is evident that the WRF model-simulated precipitation is sensitive to the physical parameterization schemes used in the model. EXPT1 and EXPT2, with the BMJ cumulus scheme, have low correlation with the IMD observed precipitation over the core monsoon region, with correlation coefficients of 0.486 and 0.366, respectively. This is due to large dry (wet) biases in the simulated precipitation in the northern (southern) parts of India (Fig. 3a,b). The corresponding experiments with the KF cumulus scheme, EXPT4 and EXPT5, have relatively high correlation coefficients of 0.681 and 0.597, thus indicating that the KF scheme shows superior performance in simulating the Indian summer monsoon precipitation under the present model setup.

The experiments with the YSU PBL scheme, EXPT1 and EXPT4, have higher correlation coefficients of 0.486 and 0.681, respectively, compared to EXPT2 (0.366) and EXPT5 (0.597) with the ACM2 PBL scheme. Though EXPT7 and EXPT10 with the ACM2 PBL scheme have higher correlation coefficients (0.778 and 0.795) compared to EXPT6 (0.730) and EXPT9 (0.699) with the YSU PBL scheme, their SD values are also large. EXPT4, EXPT12, and EXPT13, which test the suitability of shortwave radiation schemes in simulating the Indian summer monsoon precipitation, have correlation coefficients of 0.681, 0.733, and 0.708; however, EXPT12 and EXPT13 have higher SD values, indicating that the Dudhia shortwave scheme is more suitable for simulating the precipitation over the Indian region under the present model setup. EXPT9 has a smaller correlation coefficient (0.699) compared to EXPT12 (0.733); however, EXPT9, which uses the CAM longwave radiation scheme, has a smaller SD than EXPT12 with the RRTM longwave radiation scheme. Comparing the performance of other experiments testing the radiation packages in Fig. 7a, it is evident that the combination of the Dudhia shortwave radiation scheme and the RRTM longwave radiation

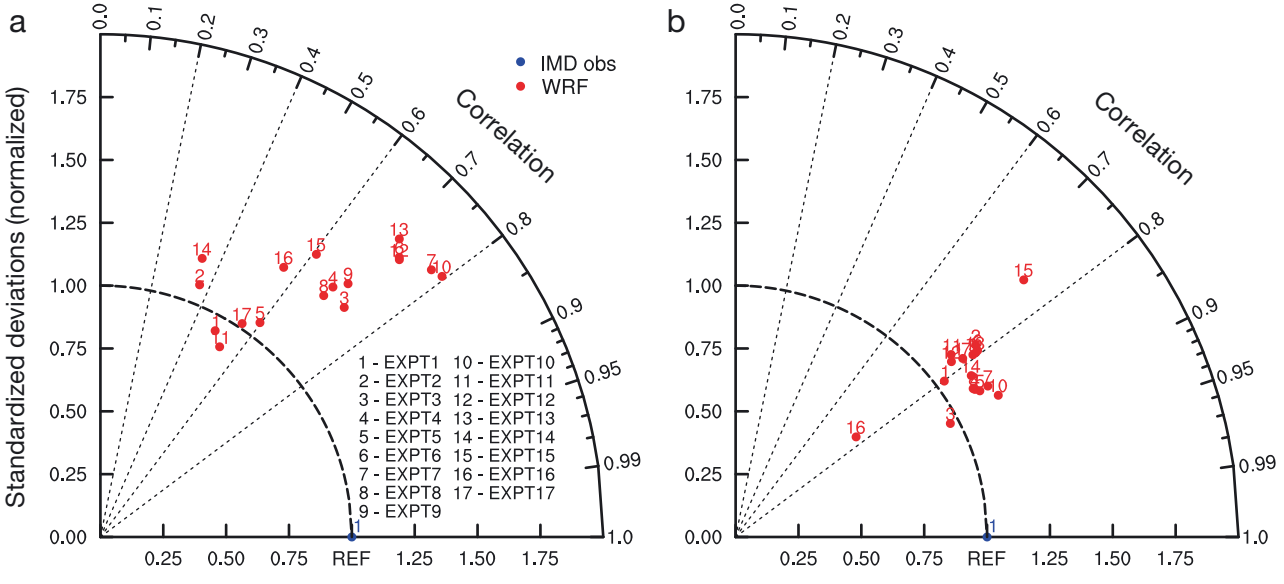

Fig. 7.(a) The IMD observed precipitation and the precipitation simulated by the WRF model experiments EXPT1 to EXPT17 over the core monsoon region. (b) Same as (a) but for 2 m air temperature

scheme performs better in simulating the precipitation over the Indian landmass during the monsoon season.

EXPT7 and EXPT10 with the WSM3 microphysical scheme have correlation coefficients of 0.778 and 0.795, while EXPT8 and EXPT11 with the WSM5 microphysical scheme have coefficients of 0.679 and 0.531. However, the model runs with WSM3 have higher SD values compared to those with the WSM5 scheme. EXPT5 with the WSM3 scheme and EXPT17 with the WSM5 scheme have comparative correlation coefficients and SD values (Fig. 7a). The precipitation simulated with the PX surface layer scheme (EXPT14) has a low correlation coefficient of 0.343 compared to that simulated by EXPT15 (0.597) with the MSS surface layer scheme. Similarly, comparing the correlation coefficients of the model experiments testing the sensitivity to land surface schemes, it is evident that the Unified Noah LSM has better skill in simulating precipitation over the Indian landmass during the monsoon season.

The Taylor diagram of the 2 m air temperature averaged over the core monsoon region (Fig. 7b) indicates that this is less sensitive to the choice of the physical parameterization schemes used in the model. All the models experiments have correlation coefficients >0.7 (Fig 7b). Except for EXPT15 and EXPT16, all the other model experiments have SD values nearer to the observed values (Fig 7b).

3.2. Intra-seasonal variability of precipitation

As is well known, the intraseasonal variations in precipitation over the Indian landmass influence the seasonal precipitation (Goswami & Ajayamohan 2001). To verify if the biases in the simulated precipitation at the seasonal time scale in the model experiments are due to biases in the simulated intraseasonal oscillations, we plotted the time evolution of the daily climatological mean precipitation (averaged over the years 1982 to 2013 and over the longitudes 70° to 90° E) over India during the JJAS season (Fig. 8). From the model-simulated daily precipitation (Fig. 8b–r) and observations (Fig. 8a), it can be seen that all the WRF model experiments simulate the seasonal cycle realistically. However, there are large differences in the magnitudes of the intraseasonal oscillations and the northward extent of the monsoon precipitation. All the model experiments except EXPT4 have frequent climatological intraseasonal oscillations with stronger magnitudes. The latitudinal extent and the climatological intraseasonal oscillations are reasonably simulated in EXPT4. In EXPT1 (Fig. 8b) and EXPT2 (Fig. 8c), the precipitation stagnates around 20° N and has a larger magnitude. These experiments have dry biases in the simulated seasonal precipitation in the northern parts of India and wet biases in the southern parts (Fig. 3a,b). EXPT3, which simulated a wet bias over the whole of India (Fig. 3c) has a stronger intraseasonal oscillation extending to 28° N (Fig. 8d). Similarly, the biases in the seasonal precipitation simulated by the other model experiments can be attributed to the biases in the lateral extent and the magnitude of the climatological intraseasonal oscillations. Using the WRF model with a domain covering the whole monsoon region and the configuration of EXPT1, Raju et al. (2015) also found the rainfall to be stagnant around 20° N, similar to that simulated in EXPT1 (Fig. 8b). This indicates that using a larger WRF domain does not necessarily lead to an improvement in the simulation of the Indian summer monsoon precipitation.

From the above analysis, it is clear that the WRF model simulations of the Indian summer precipitation are sensitive to the physical parameterization schemes used. The results also indicate that it is essential to choose the correct combination of physical parameterization schemes. Among the experiments performed in this study, EXPT4 not only has smaller RMSE and biases in the simulated precipitation over the core monsoon region but also shows reasonable simulation of the climatological intraseasonal oscillations.

3.3. Interannual variability of seasonal precipitation and 2 m air temperature anomalies

In this analysis, we averaged the seasonal precipitation anomalies simulated by all the WRF model experiments over the core monsoon region and normalized the time series by their SD to verify the accuracy of the WRF model in simulating the interannual variability of the Indian summer monsoon precipitation. The normalized precipitation anomalies are shown in Fig. 9. From the normalized time series (Fig. 9), it is evident that the simulation of the interannual variability in precipitation is sensitive to the choice of the physical parameterization scheme in the WRF model. The ENSO and IOD influence the inter-annual variability in the Indian summer monsoon (Fig. 9), with El Niño almost always resulting in reduction of the seasonal precipitation over the Indian landmass. In fact, the years with a large deficiency (SD < 1) of rainfall over India are coincident

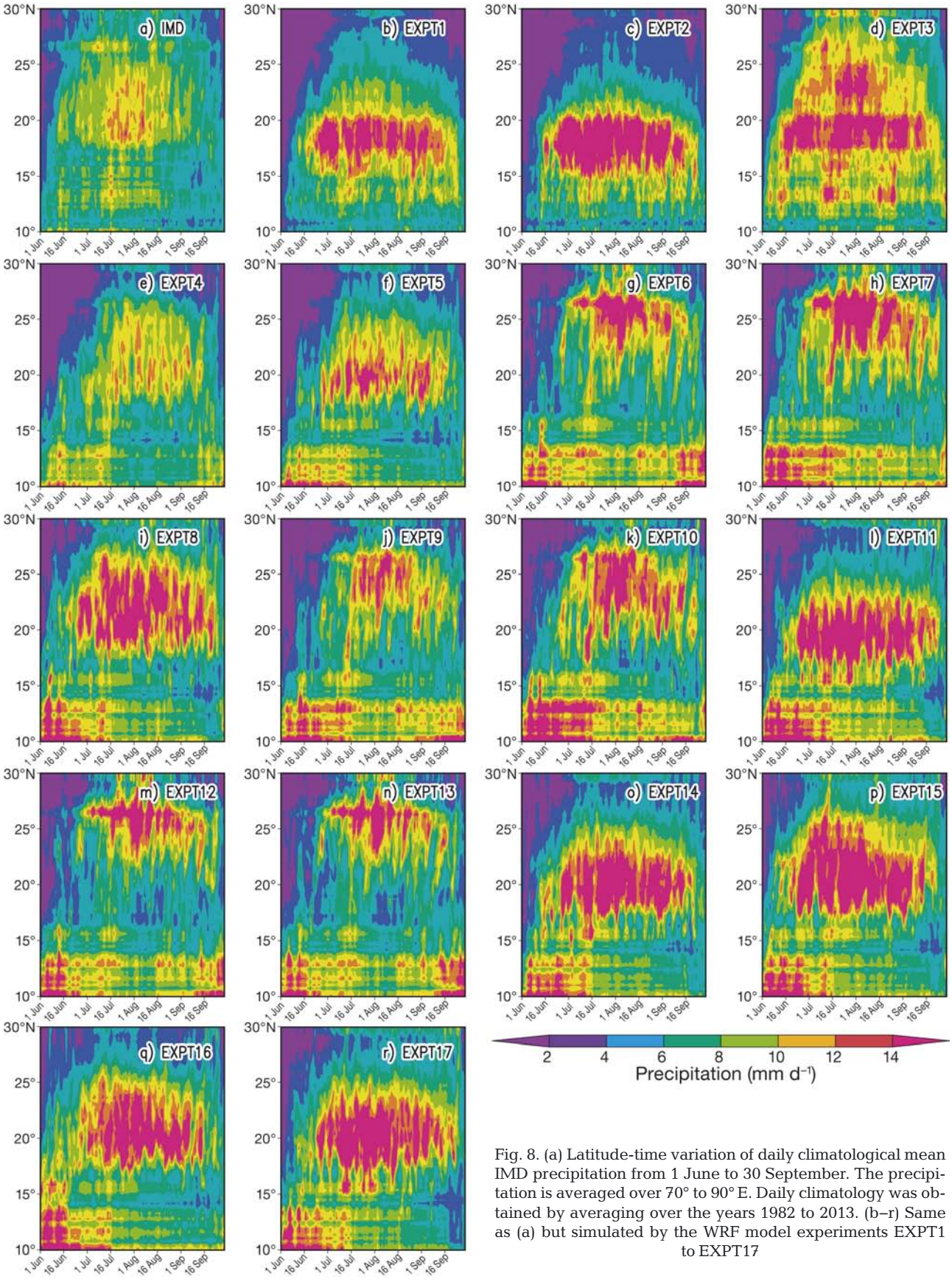

Fig. 8. (a) Latitude-time variation of daily climatological mean IMD precipitation from 1 June to 30 September. The precipitation is averaged over 70° to 90° E. Daily climatology was obtained by averaging over the years 1982 to 2013. (b–r) Same as (a) but simulated by the WRF model experiments EXPT1 to EXPT17

with the El Niño years (Fig. 9). Most of the WRF model experiments could capture extreme deficient rainfall years realistically, though with variation in the amplitude of the precipitation anomalies (Fig. 9). The years with precipitation anomalies >1 SD (1983, 1994, 2006, 2013) are either positive Indian Ocean Dipole (PIOD) years or ENSO neutral years (Fig. 9). As evident from Fig. 9, pure PIOD years (1983, 1994, 2006, 2008, 2012) are generally associated with higher precipitation over the Indian region. The PIOD in 1982 and 1997, which co-occurred with El Niño, reduced the effects of El Niño on the Indian summer monsoon precipitation. Most of the WRF model experiments could realistically capture the phase of the precipitation anomalies during the extreme precipitation years (Fig. 9). La Niña (1988, 2007, 2010, 2011) and negative Indian Ocean Dipole (NIOD) years (1992, 1996) have positive precipitation anomalies over the Indian landmass (Fig. 9).

We plotted the spatial distribution of the composite precipitation anomalies during the PIOD and El Niño years of 3 model experiments, EXPT4, EXPT10, and EXPT14, to understand the differences in the spatial distribution of the precipitation anomalies among the model experiments (Fig. 10). EXPT4 simulated monsoon precipitation with smaller biases over the core monsoon region and has reasonable correlation with the IMD observed precipitation (correlation coefficient of 0.681; Fig. 7a), whereas EXPT10 simulated precipitation with large wet biases over the Indian landmass and has a correlation coefficient of 0.795 over the core monsoon regions and a high SD. EXPT14 has the smallest correlation coefficient of 0.343 and also a lower SD than the other 2 experiments. These experiments are representative of the extremes in the simulated precipitation within the model experiments and, hence, are good candidates for understanding the spatial distribution of the precipitation during extreme events.

The spatial distribution of the precipitation anomalies composited over the pure PIOD seasons (JJAS of 1983, 1994, 2006, 2008, and 2012) shows significant positive anomalies over northwest India and the eastern parts of central India (Fig. 10a; shaded). These are due to the cyclonic vertically integrated moisture flux anomalies (Behera et al. 1999) over the region (Fig. 10a; vectors). During pure PIOD events, the northeastern parts of India experience a significant reduction in precipitation (Fig. 10a). The composite 2 m air temperature anomalies during the pure PIOD events show negative anomalies over the northwestern parts of India and positive anomalies over the northeastern parts (Fig. 10i). The areas of

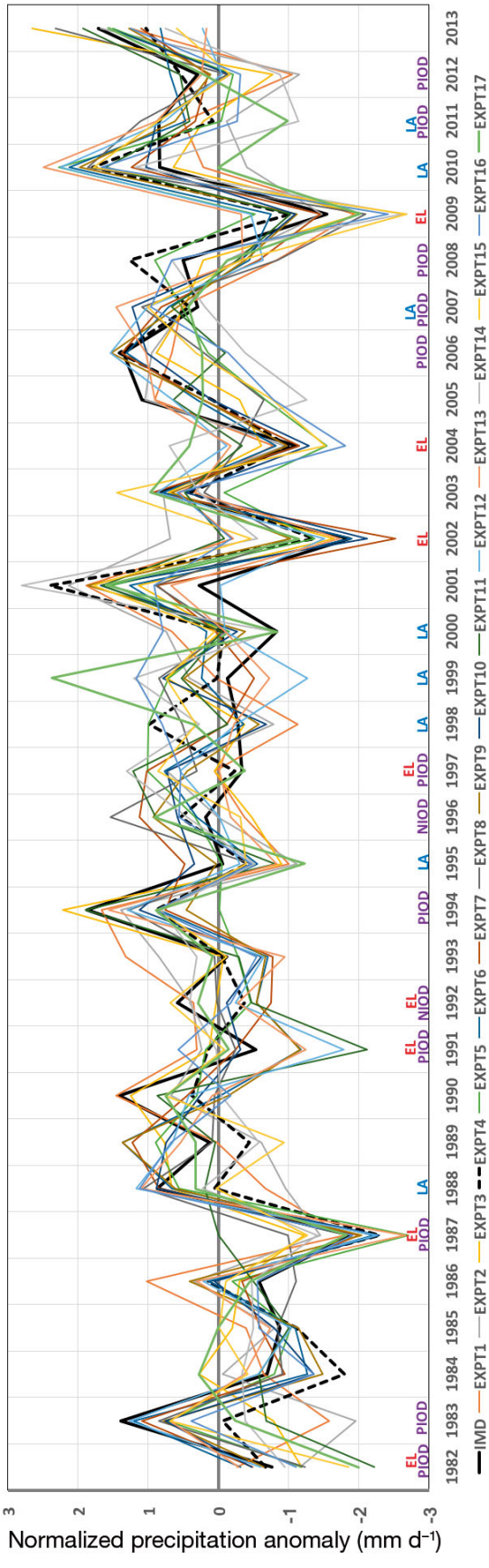

Fig. 9. Interannual variation of the normalized seasonal precipitation anomalies over the core monsoon region of the IMD observed precipitation and the precipitation simulated by the WRF model experiments EXPT1 to EXPT17. EL: El Niño; PIOD: positive Indian Ocean Dipole; LA: La Niña; NIOD: negative Indian Ocean Dipole

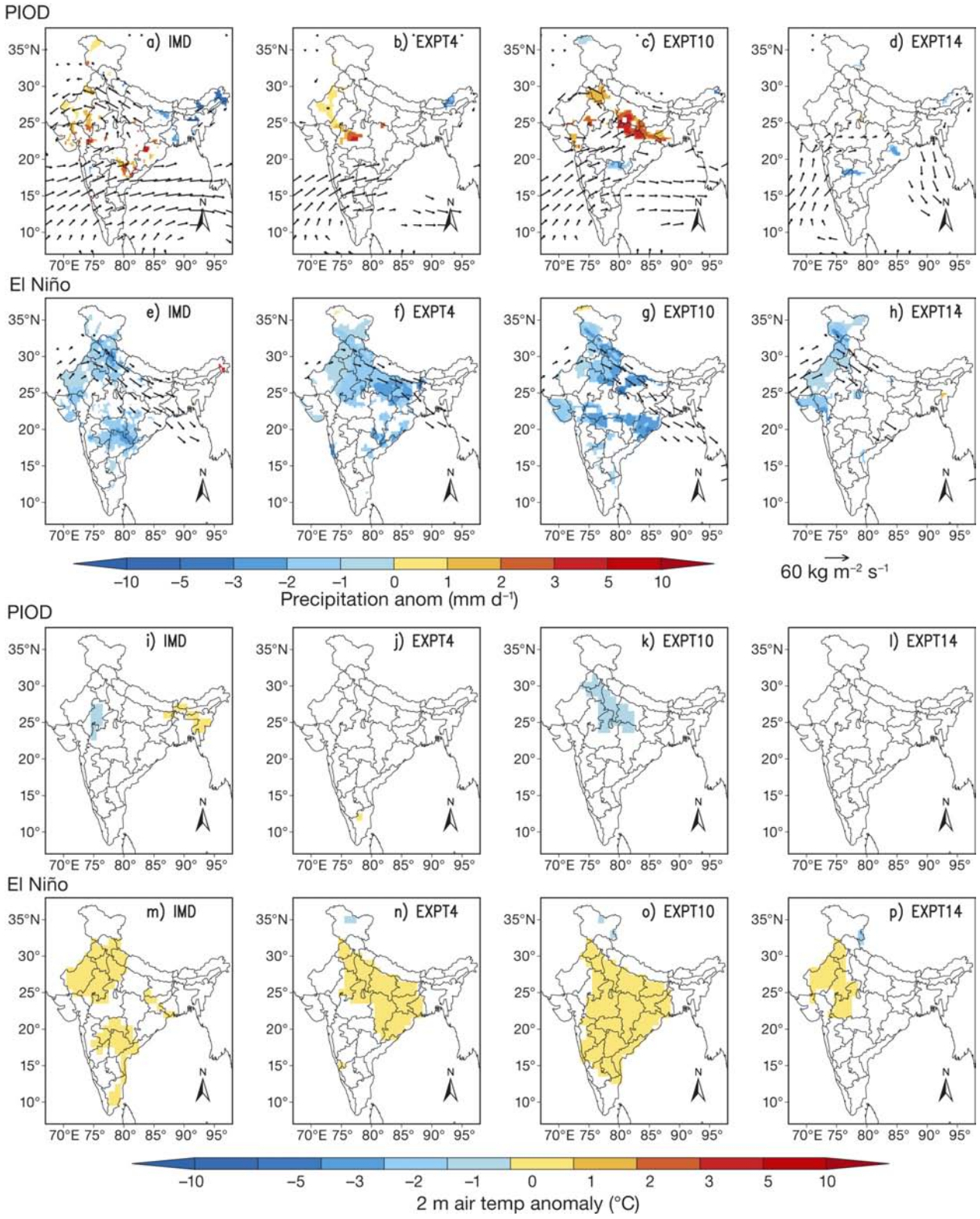

Fig. 10. (a–d) Composite of JJAS seasonal precipitation anomalies observed during pure PIOD years and simulated by WRF model experiments EXPT4, EXPT10, and EXPT14, respectively. (e–h) Same as (a–d) but during El Niño years. (i–l) Composite JJAS seasonal 2 m air temperature anomalies (°C) observed during pure PIOD years and simulated by WRF model experiments EXPT4, EXPT10, and EXPT14, respectively. (m–p) Same as (i–l) but during El Niño years. Vectors in (a–h) are the vertically integrated moisture flux anomalies. Only significant values are plotted. Significance was tested using Student's 2-tailed *t*-test at 90% confidence level

positive (negative) 2 m air temperature anomalies coincide with the regions of negative (positive) precipitation anomalies observed over the Indian landmass. EXPT4 was able to capture the spatial distribution of precipitation anomalies realistically (Fig. 10b), with significant positive anomalies over the northwestern parts of India and significant negative anomalies over the northeastern parts during the pure PIOD events. However, the 2 m air temperatures simulated by EXPT4 are significant only over a small region of southern India (Fig. 10j). EXPT4 also had difficulty in simulating the cyclonic vertically integrated moisture flux anomalies over the Indian landmass (Fig. 10b). EXPT10 simulated large areas of significant positive precipitation anomalies over the northern parts of the Indian landmass during the pure PIOD events (Fig. 10c) that were associated with significant intense cyclonic vertically integrated moisture flux anomalies over the landmass (Fig. 10c; vectors). The 2 m air temperature anomalies simulated by EXPT10 are significantly negative over the northern parts of India (Fig. 10k) and EXPT14 simulated negative precipitation anomalies over scattered regions of central India associated with anticyclonic moisture flux anomalies over the landmass (Fig. 10d) during the positive PIOD events. EXPT14 also had difficulty in simulating a realistic 2 m air temperature distribution over the landmass during the pure PIOD events (Fig. 10l).

El Niño has a stronger influence on the Indian summer monsoon precipitation compared to PIOD events (Fig. 10a), as is evident from the composite (mean of JJAS 1982, 1987, 1991, 1997, 2002, 2004, and 2009) El Niño events (Fig. 10e). Significant negative precipitation anomalies are spread over the entire core monsoon region during the El Niño events (Fig. 10e) and are associated with significant anticyclonic moisture flux anomalies over the landmass (Fig. 10e; vectors). Both EXPT4 (Fig. 10f) and EXPT10 (Fig. 10g) were able to realistically simulate the spatial distribution of precipitation as well as the moisture flux anomalies. However, EXPT10-simulated anomalies (Fig. 10g) are higher in magnitude compared to the observed anomalies (Fig. 10e). EXPT14 simulated significant negative precipitation anomalies confined to northwestern parts of India (Fig. 10h). Significant positive 2 m air temperature anomalies can be seen over large parts of the Indian landmass during the El Niño events (Fig. 10m). Similar to the simulation of precipitation anomalies, EXPT4 (Fig. 10n) and EXPT10 (Fig. 10o) realistically simulated the 2 m air temperature anomalies, with EXPT10-simulated anomalies (Fig. 10o) covering larger areas of the Indian landmass compared to the observed spatial distribution of the anomalies (Fig. 10m). EXPT14-simulated 2 m air temperature anomalies are significant only over the northwestern parts of India (Fig. 10p). In summary, EXPT4 has a suitable combination of schemes to simulate the spatial distribution of the precipitation anomalies during PIOD and El Niño events.

4. CONCLUSIONS

We carried out a set of 17 experiments using various combinations of physical parameterization schemes in the WRF model to simulate the Indian summer monsoon precipitation and 2 m air temperature. The experiments were designed to select a suitable combination of physical parameterization schemes for simulating the spatial and temporal distribution of the precipitation and 2 m air temperature realistically. The experiments were formulated to test 2 cumulus parameterization schemes, KF and BMJ, 4 shortwave radiation schemes, 3 longwave radiation schemes, 2 planetary boundary layer schemes, 2 microphysical schemes, 2 surface layer schemes, and 3 land-surface models (Tables 1 & 2).

The analysis of the results indicates that the WRF model-simulated precipitation is sensitive to the physical parameterization schemes used in the model and that choosing the correct combination is essential for simulating the summer monsoon precipitation over the Indian landmass. The tests with different cumulus schemes found the KF scheme to be more suitable for simulating the boreal summer precipitation over the Indian landmass compared to the BMJ scheme. The KF scheme simulations have smaller biases in the spatial and temporal distribution of the precipitation compared to the model runs with the BMJ scheme. The model experiments (EXPT1 and EXPT2) with the BMJ scheme have wet (dry) biases in the simulated precipitation over the southern (northern) parts of India, due to cyclonic biases in the vertically integrated moisture fluxes over the southern parts of India. The climatological intraseasonal oscillations of precipitation are stagnant over the southern parts of India in the BMJ simulations (EXPT1 and EXPT2) resulting in wet biases over southern India in the seasonal mean. However, the experiments with the KF scheme, EXPT4 and EXPT5, have smaller biases over the core monsoon region and the intraseasonal oscillations are more realistic than those simulated with the BMJ scheme. Interestingly, the spatial distribution of the precipita-

tion biases in EXPT3 with the BMJ scheme is different from those of EXPT1 and EXPT2, with EXPT3 simulating wet biases over most parts of the Indian landmass whereas EXPT1 and EXPT2 have a dipole structure in the distribution of the biases. Similarly, EXPT4 to EXPT17, which use the KF scheme, show differences in the spatial as well as temporal distribution of the biases in precipitation, thereby demonstrating that choosing the correct combination of physical schemes is required for simulating the precipitation over the Indian landmass during the boreal summer season.

The results of experiments with different PBL schemes indicate that the YSU PBL scheme performs better in simulating the Indian summer monsoon precipitation compared to the ACM2 PBL scheme. The ACM2 PBL scheme simulated a more unstable atmosphere resulting in an enhancement in the wet biases over the Indian landmass. However, the results produced by different PBL schemes do not differ as much as those resulting from different cumulus schemes. The model experiments indicate that the radiation package with the Dudhia shortwave radiation and RRTM longwave radiation schemes simulate precipitation over the Indian landmass with smaller biases compared to the CAM and RRTMG radiation packages. Of the 2 microphysical schemes we tested, the WSM3 scheme simulated a more realistic distribution of the precipitation compared to the WSM5 scheme. The simulated precipitation was also found to be sensitive to the surface layer scheme as well as the land surface model. The MSS surface layer scheme and the Unified Noah LSM were found to be suitable for simulating the Indian summer monsoon.

The interannual variability of the monsoon precipitation over the core monsoon regions was simulated realistically in the model experiments; however, the simulated variability was dependent on the physical parameterization schemes used in the model. Of all the model experiments tested, we find the experimental setup of EXPT4, with the KF cumulus, Dudhia shortwave, RRTM longwave, YSU PBL, WSM3 microphysics, and MSS surface layer schemes, and the Unified Noah LSM to be suitable for simulating the Indian summer monsoon precipitation realistically.

The 2-tier approach of specifying the sea-surface temperature to the forecasting models often results in overestimation of precipitation (Kumar et al. 2005). As shown by Ratnam et al. (2009), the 1-tier approach of using a regional coupled model can improve the simulation of intraseasonal as well as interannual variability of Indian summer precipitation. We are now planning such a regional coupled model with the combination of EXPT4 physical parameterization schemes to generate downscaled forecasts over India in the future, with SINTEX-F2v (Doi et al. 2016) CGCM forecasts as the boundary conditions.

Acknowledgements. The authors thank 2 anonymous reviewers for their comments which substantially improved the manuscript. This research is supported by JSPS KAKENHI Grant Numbers 16H04047 and 16K17810. The authors thank the India Meteorological Department for providing the gridded precipitation and 2 m air temperature data. The ERA-Interim data was obtained from the ECMWF data server.

LITERATURE CITED

Annamalai H, Slingo JM (2001) Active/break cycles: diagnosis of the intraseasonal variability of the Asian summer monsoon. Clim Dyn 18:85–102

Argueso D, Hidalgo-Munoz J, Gamiz-Fortis SR, Esteban-Parra MJ, Dudhia J, Castro-Diez Y (2011) Evaluation of WRF parameterizations for climate studies over southern Spain using a multistep regionalization. J Clim 24: 5633–5651

Behera SK, Krishnan R, Yamagata T (1999) Unusual ocean-atmosphere conditions in the tropical Indian Ocean during 1994. Geophys Res Lett 26:3001–3004

Betts AK, Miller MJ (1986) A new convective adjustment scheme. II. Single column tests using GATE wave, BOMEX and arctic air-mass data sets. QJR Meteorol Soc 112:693–709

Bhaskar Rao DV, Ratna SB, Srinivas D (2013) An assessment of cumulus parameterization schemes in the short-range prediction of rainfall during the onset phase of the Indian southwest monsoon using MM5 model. Atmos Res 120-121:249–267

Bhaskaran B, Jones RG, Murphy JM, Noguer M (1996) Simulations of the Indian summer monsoon using a nested climate model: domain size experiments. Clim Dyn 12: 573–587

Chen TC, Chen JM (1993) The 10–20-day model of the 1979 Indian monsoon: its relation with the time variation of monsoon rainfall. Mon Weather Rev 121:2465–2482

Chou MD, Suarez MJ (1999) A solar radiation parameterization for atmospheric studies. NASA Tech Memo 104606, 15

Collins WD, Rasch PJ, Boville BA, Hack JJ and others (2004) Description of the NCAR Community Atmosphere Model (CAM3.0). NCAR Tech Note NCAR/TN-464+STR

Correia J Jr, Arritt RW, Anderson CJ (2008) Idealized mesoscale convective system structure and propagation using convective parameterization. Mon Weather Rev 136: 2422–2442

Crétat J, Pohl B, Richard Y, Drobinski P (2012) Uncertainties in simulating regional climate of Southern Africa: sensitivity to physical parameterizations using WRF. Clim Dyn 38:613–634

Dash SK, Shekhar MS, Singh GP (2006) Simulation of Indian summer monsoon circulation and rainfall using RegCM3. Theor Appl Climatol 86:161–172

Dash SK, Pattnayak KC, Panda SK, Vaddi D, Mamgain A (2015) Impact of domain size on the simulation of Indian summer monsoon in RegCM4 using mixed convection

scheme and driven by HadGEM2. Clim Dyn 44:961–975
Dee DP, Uppala SM, Simmons AJ, Berrisford P and others (2011) The ERA-Interim reanalysis: configuration and performance of the data assimilation system. QJR Meteorol Soc 137:553–597
Dickinson RE, Errico RM, Giorgi F, Bates GT (1989) A regional climate model for the western United States. Clim Change 15:383–422
Doi T, Behera SK, Yamagata T (2016) Improved seasonal prediction using the SINTEX-F2 coupled model. J Adv Model Earth Syst 8:1847–1867
Dudhia J (1989) Numerical study of convection observed during the winter monsoon experiment using a mesoscale two-dimensional model. J Atmos Sci 46:3077–3107
Dudhia J (1996) A multi-layer soil temperature model for MM5. Preprints, Sixth PSU/NCAR Mesoscale Model Users' Workshop, Boulder CO, 22–24 Jul 1996, National Center for Atmospheric Research, p 49–50. www2.mmm.ucar.edu/wrf/users/phys_refs/LAND_SURFACE/5_layer_thermal.pdf (accessed 19 October 2017)
Dudhia J (2016) Overview of WRF physics. WRF Tutorial 2016 presentation. www2.mmm.ucar.edu/wrf/users/tutorial/201607/physics.pdf (accessed 19 October 2017)
Evans JP, Ekström M, Ji F (2012) Evaluating the performance of a WRF physics ensemble over South-East Australia. Clim Dyn 39:1241–1258
Giorgi F, Bates GT (1989) The climatological skill of a regional model over complex terrain. Mon Weather Rev 117:2325–2347
Goswami BN (2005) South Asian monsoon. In: Lau WKM, Waliser DE (eds) Intraseasonal variability in the atmosphere-ocean climate system. Springer, Berlin, p 19–55
Goswami BN, Ajaya Mohan RS (2001) Intraseasonal oscillations and interannual variability of the Indian summer monsoon. J Clim 14:1180–1198
Hong SY, Dudhia J, Chen SH (2004) A revised approach to ice microphysical processes for bulk parameterization of cloud and precipitation. Mon Weather Rev 132:103–120
Hong SY, Noh Y, Dudhia J (2006) A new vertical diffusion package with an explicit treatment of entrainment processes. Mon Weather Rev 134:2318–2341
Iacono MJ, Delamere JS, Mlawer EJ, Shephard MW, Clough SA, Collins WD (2008) Radiative forcing by long-lived greenhouse gases: calculations with the AER radiative transfer models. J Geophys Res 113:D13103
Jacob D, Podzum R (1997) Sensitivity studies with the regional climate model REMO. Meteorol Atmos Phys 63: 119–129
Janjic ZI (1994) The step-mountain eta coordinate model: further developments of the convection, viscous sublayer and turbulence closure schemes. Mon Weather Rev 122: 927–945
Juang HMH, Hong SY, Kanamitsu M (1997) The NCEP spectral model: an update. Bull Am Meteorol Soc 78: 2125–2143
Kain JS (2004) The Kain–Fritsch convective parameterization: An update. J Appl Meteorol 43:170–181
Kala J, Andrys J, Lyons TJ, Foster IJ, Evans BJ (2015) Sensitivity of WRF to driving data and physics options on a seasonal time-scale for the southwest of Western Australia. Clim Dyn 44:633–659
Krishnamurti TN, Ardunay P (1980) The 10 to 20 day westward propagating mode and 'breaks' in the monsoon. Tellus 32:15–26
Krishnamurti TN, Bhalme HN (1976) Oscillations of a monsoon system. I. Observational aspects. J Atmos Sci 33: 1937–1954
Krishnamurti TN, Jayakumar P, Sheng J, Surgi N, Kumar A (1985) Divergent circulations of the 30–50 day time scale. J Atmos Sci 42:364–375
Krishnan R, Swapna P (2009) Significant influence of the boreal summer monsoon flow on the Indian Ocean response during dipole events. J Clim 22:5611–5634
Krishnan R, Zhang C, Sugi M (2000) Dynamics of breaks in the Indian summer monsoon. J Atmos Sci 57:1354–1372
Krishnan R, Ayantika DC, Kumar V, Pokhrel S (2011) The long-lived monsoon depressions of 2006 and their linkage with the Indian Ocean Dipole. Int J Climatol 31: 1334–1352
Kumar KK, Hoerling M, Rajagopalan B (2005) Advancing dynamical prediction of Indian monsoon rainfall. Geophys Res Lett 32:L108704
Lucas-Picher P, Christensen JH, Saeed F, Kumar P and others (2011) Can regional climate models represent the Indian monsoon? J Hydrometeorol 12:849–868
Maharana P, Dimri AP (2016) Study of intraseasonal variability of Indian summer monsoon using a regional climate model. Clim Dyn 46:1043–1064
Mlawer E, Steven J, Taubman J, Brown PD, Iacono MJ, Clough SA (1997) Radiative transfer for inhomogeneous atmospheres: RRTM, a validated correlated-k model for the longwave. J Geophys Res 102:16663–16682
Mooney PA, Mulligan FJ, Fealy R (2013) Evaluation of the sensitivity of the weather research and forecasting model to parameterization schemes for regional climates of Europe over the period 1990–95. J Clim 26:1002–1017
Mukhopadhyay P, Taraphdar S, Goswami BN, Krishnakumar K (2010) Indian summer monsoon precipitation climatology in a high resolution regional climate model: impact of cumulus parameterization schemes on systematic biases. Weather Forecast 25:369–387
Murakami M (1976) Analysis of summer monsoon fluctuations over India. J Meteorol Soc Jpn 54:15–31
Murakami T, Chen LX, Xie A (1984) On the 40–50 day oscillations during the 1979 northern hemisphere summer. I. Phase propagation. J Meteorol Soc Jpn 62:440–468
Nakazawa T (1986) Mean features of 30–60 day variations as inferred from 8-year OLR data. J Meteorol Soc Jpn 64: 777–786
Pai DS, Sridhar L, Rajeevan M, Sreejith OP, Satbhai NS, Mukopadhyay B (2014) Development of a new high spatial resolution long period daily gridded rainfall data set over India and comparison with existing data over the region. Mausam (New Delhi) 65:1–18
Paulson CA (1970) The mathematical representation of wind speed and temperature profiles in the unstable atmospheric surface layer. J Appl Meteorol 9:857–861
Pleim JE (2006) A simple, efficient solution of flux-profile relationships in the atmospheric surface layer. J Appl Meteorol Climatol 45:341–347
Pleim JE (2007) A combined local and nonlocal closure model for the atmospheric boundary later. I. Model description and testing. J Appl Meteorol Climatol 46: 1383–1395
Pleim JE, Xiu A (2003) Development of a land surface model. II. Data assimilation. J Appl Meteorol 42:1811–1822
Raghavan K (1973) Break-monsoon over India. Mon Weather Rev 101:33–43
Rajeevan M, Gadgil S, Bhate J (2010) Active and break spells of the Indian summer monsoon. J Earth Syst Sci 119:

229–247

Raju A, Parekh A, Chowdary JS, Gnanaseelan C (2015) Assessment of the Indian summer monsoon in the WRF regional climate model. Clim Dyn 44:3077–3100

Ramamurthy K (1969) Monsoon of India: some aspects of the 'break' in the Indian southwest monsoon during July and August (forecasting manual, Part IV.18.3). India Meteorological Department, New Delhi. www.imdpune.gov.in/Weather/reports.html

Ratnam JV, Cox EA (2006) Simulation of monsoon depressions using MM5: sensitivity to cumulus parameterization schemes. Meteorol Atmos Phys 93:53–78

Ratnam JV, Kumar KK (2005) Sensitivity of the simulated monsoons of 1987 and 1988 to convective parameterization schemes in MM5. J Clim 18:2724–2743

Ratnam JV, Giorgi F, Kaginalkar A, Cozzini S (2009) Simulation of the Indian monsoon using the RegCM3-ROMS regional coupled model. Clim Dyn 33:119–139

Saji NH, Goswami BN, Vinayachandran PN, Yamagata T (1999) A dipole mode in the tropical Indian Ocean. Nature 401:360–363

Shrivastava R, Dash SK, Oza RB, Sharma DN (2014) Evaluation of parameterization schemes in WRF model for estimation of mixing height. Int J Atmos Sci 2014:451578

Skamarock WC, Klemp JB, Dudhia J, Gill DO and others (2008) A description of the Advanced Research WRF version 3. NCAR Tech Note TN-475+STR (www2.mmm.ucar.edu/wrf/users/docs/arw_v3.pdf)

Srinivas CV, Hariprasad D, Rao DVB, Anjaneyulu Y, Baskaran R, Venkatraman B (2013) Simulation of the Indian summer monsoon regional climate using advanced research WRF model. Int J Climatol 33:1195–1210

Srinivasan J, Smith GL (1996) The role of heat fluxes and moist static energy in tropical convergence zones. Mon Weather Rev 124:2089–2099

Srivatsava AK, Rajeevan M, Kshirsagar SR (2009) Development of a high resolution daily gridded temperature data set (1969-2005) for the Indian region. Atmos Sci Lett 10: 249–254

Tewari M, Chen F, Wang W, Dudhia J and others (2004) Implementation and verification of the unified NOAH land surface model in the WRF model. 20th Conf on weather analysis and forecasting/16th Conf on numerical weather prediction, pp 11–15. www2.mmm.ucar.edu/wrf/users/phys_refs/LAND_SURFACE/noah.pdf (last accessed 19 October 2017)

Umakanth U, Kesarkar AP, Raju A, Rao SVB (2016) Representation of monsoon intraseasonal oscillations in regional climate model: sensitivity to convective physics. Clim Dyn 47:895–917

Vellore RK, Krishnan R, Pendharkar J, Choudhury AD, Sabin TP (2014) On the anomalous precipitation enhancement over the Himalayan foothills during monsoon breaks. Clim Dyn 43:2009–2031

Vernekar AD, Ji Y (1999) Simulation of the onset and intraseasonal variability of two contrasting summer monsoons. J Clim 12:1707–1725

Yuan X, Liang XZ, Wood E (2012) WRF ensemble downscaling seasonal forecasts of China winter precipitation during 1982–2008. Clim Dyn 39:2014–2058

Editorial responsibility: Filippo Giorgi, Trieste, Italy

Submitted: April 3, 2017; Accepted: Juli 13, 2017
Proofs received from author(s): October 19, 2017